





Phytochemical Isolation and Antimicrobial, Thrombolytic, Anti-inflammatory, Analgesic, and Antidiarrheal Activities from the Shell of Commonly Available *Citrus reticulata* Blanco: Multifaceted Role of Polymethoxyflavones

Nutrition and Metabolic Insights
Volume 18: 1–34
© The Author(s) 2025
Article reuse guidelines:
sagepub.com/journals-permissions
DOI: 10.1177/11786388251327668


Md. Jamal Hossain¹, Md. Abdus Samadd², Mst. Nusrat Zahan Urmi¹,
Mst. Farzana Yeasmin Reshmi¹, Md. Shohel Hossen¹
and Mohammad A. Rashid²

¹Department of Pharmacy, School of Pharmaceutical Sciences, State University of Bangladesh, Dhaka, Bangladesh. ²Department of Pharmaceutical Chemistry, Faculty of Pharmacy, University of Dhaka, Dhaka, Bangladesh.

ABSTRACT: Fruit wastes are becoming popular as treasures for drug discovery in different classes of therapeutics. This research aimed to investigate the phytochemicals and potential bioactivities, such as antimicrobial, thrombolytic, anti-inflammatory, analgesic, and antidiarrheal properties of commonly available mandarin orange (*Citrus reticulata* Blanco) peel through experimental and computational techniques. Extensive chromatographic and ¹H-NMR spectroscopic analysis was employed to isolate four purified compounds, which were characterized as tangeretin (A), nobiletin (B), limonin (C), and β-sitosterol (D). Furthermore, GC-MS/MS analysis detected over 90 compounds with a notable number of polymethoxyflavones, including nobiletin (29.04%), tangeretin (15.55%), artemetin (8.1%), 6-demethoxytangeretin (1.28%), sinensetin (0.95%), demethylnobiletin (0.14%), pebrellin (0.10%), and salvigenin (0.04%). Dichloromethane soluble fraction (DCMSF) exerted the highest antimicrobial potency *Candida albicans* against (20mm zone of inhibition) in the disk diffusion assay method. The aqueous soluble fraction (AQSF) exhibited 34.71% and 48.14% inhibition in hypotonic solution-induced and heat-induced hemolysis in the membrane stabilizing assay. Similarly, the AQSF exhibited the highest anti-thrombotic property with 32.57% clot lysis. The investigated 3 doses of the methanolic extracts (100, 200, and 400mg/kg body weight) exerted statistically significant *in vivo* central analgesic effects in a tail-flicking method in a time-dependent manner. Moreover, all the doses exhibited significant efficacy in inhibiting acetic acid-induced abdominal writhing and castor oil-induced diarrheal episodes in mouse models. The molecular docking studies corroborated the existing *in vitro* and *in vivo* findings by demonstrating better or comparable binding affinities toward the respective receptors and favorable pharmacokinetic properties and toxicological profiles. The present findings indicate that *C. reticulata* is a rich source of polymethoxyflavones, demonstrating potential efficacy against microbial infections, thrombosis, inflammation, pain, and diarrhea. Nonetheless, comprehensive phytochemical screening is imperative to identify additional bioactive compounds and evaluate their pharmacological effects against several chronic health conditions, grounded in their traditional uses and current evidence.

KEYWORDS: Mandarin orange (*Citrus reticulata* Blanco), phytochemical isolation, NMR, GC-MS/MS analysis, antimicrobial properties, anti-inflammatory, analgesics, antidiarrheal

RECEIVED: September 11, 2024. **ACCEPTED:** February 26, 2025.

TYPE: Original Research

FUNDING: The author(s) received no financial support for the research, authorship, and/or publication of this article.

DECLARATION OF CONFLICTING INTERESTS: The author(s) declared no potential conflicts of interest with respect to the research, authorship, and/or publication of this article.

CORRESPONDING AUTHOR: Md. Jamal Hossain, Department of Pharmacy, School of Pharmaceutical Sciences, State University of Bangladesh, South Purbachal, Dhaka 1461, Bangladesh. Email: jamal.du.p48@gmail.com

Introduction

The investigation of contemporary synthetic medications is approached with caution due to their known adverse effects.¹ In contrast, conventional herbals are obtaining popularity as they are perceived as environmentally friendly, more natural, and fewer adverse effects.² So, despite all of the benefits of existing synthetic medications, scientists carry on to favor nature-based remedies.³ The unique phytoconstituents of various plant parts contribute to the diverse potential of medicinal species, functional foods, or food byproducts in alleviating and treating various human disorders.^{3–5} In Indian culture, approximately 80 000 species of medicinal plants have been utilized as traditional medication since ancient times.⁶ Plant-based medications serve as the primary resource for medical care for a substantial portion of the global population.^{7–9}

Particularly in low-income nations, where facilities are limited, traditional therapy and ethnic values play a significant role, making natural remedies an affordable choice for essential healthcare.^{10,11}

Mandarin fruit (*Citrus reticulata* Blanco), a wide species that belongs to the family Rutaceae valued not only for its appealing flavor but also for its numerous therapeutic properties, including anticancer, antioxidant, anti-hyperlipidemic, anti-inflammatory, and antidiabetic effects.^{12,13} These health benefits are attributed to the rich presence of phytochemicals such as organic acids, carotenoids, sugars, amino acids, flavonoids, polyphenols, limonoids, and phenolic acids in mandarin fruit.¹³ The traditional uses of mandarin fruit extend to laxative, aphrodisiac, antiemetic, astringent, and tonic properties, as well as skin-related benefits.^{14–16} It is also used as a stomachic



Creative Commons Non Commercial CC BY-NC: This article is distributed under the terms of the Creative Commons Attribution-NonCommercial 4.0 License (<https://creativecommons.org/licenses/by-nc/4.0/>) which permits non-commercial use, reproduction and distribution of the work without further permission provided the original work is attributed as specified on the SAGE and Open Access pages (<https://us.sagepub.com/en-us/nam/open-access-at-sage>).

and carminative.^{15,17,18} The pericarp and endocarp possess medicinal qualities, which are employed in the treatment and management of various conditions such as analgesia, anticholesterolemia, anti-inflammatory, antiseptic, anti-asthmatic, carminative, antiscorbutic, expectorant, antitussive, and stomachic.^{18,19} The immature green exocarp is utilized for alleviating, gastrointestinal distension, liver cirrhosis, liver, hypochondrium, spleen enlargement, as well as chest pains. The seed exhibits carminative and analgesic properties, making it a remedy for hernias, mastitis, lumbago, and discomfort or enlargement of the testicles.¹⁹

In addition to its extensive biological significance, some phytochemical studies revealed that *C. reticulata* is a treasure trove of bioactive substances. Another report indicates that polymethoxyflavones (PMFs) are plentiful in citrus peels, particularly in mature citrus peels. These peels have been traditionally employed in Chinese medicine for numerous years to alleviate various conditions, including stomach upset, skin inflammation, cough, ringworm infections, muscle pain, and possibly lowering blood pressure.^{20,21}

The current study utilizes Gas Chromatography-Mass Spectrometry (GC-MS) and NMR spectroscopy to identify and isolate bioactive components from methanolic extract of *C. reticulata* fruits peel. This research additionally explored the antimicrobial, anti-inflammatory, thrombolytic, central and peripheral analgesic, and anti-diarrheal properties of this species. The outcomes may be helpful to create a new way to discover new drugs and enhance the nutraceuticals and medicinal values of this very commonly available fruit peel waste of the *C. reticulata*.

Methods and Materials

Sample collection and drying

In July 2023, Mandarin oranges (*Citrus reticulata* Blanco) were procured from the West Dhanmondi local market in Dhaka, Bangladesh. The batch originated from the Yunnan region in southwest China. Following the purchase from the market, the procedure involved manually collecting the fresh peels and subsequently washing them with fresh water. The drying process was facilitated by prolonged exposure to open air. Strict protocols were employed to ensure that the ambient temperature remained below 30°C during the drying regimen. This precaution was taken to prevent any potential degradation and to ensure the preservation of heat-sensitive compounds. The dried fresh peels of *C. reticulata* are depicted in supplementary Figure S1.

Chemicals and reagents

Analytical-grade reagents and substances were employed in the study. Tween 80 and the suspending medium for the extract were procured from Merck (Germany). Glibenclamide, normal saline solution, and loperamide were supplied by BEXIMCO

Pharmaceuticals Ltd., Dhaka, Bangladesh (Additional chemicals included aspirin, diclofenac sodium, and sodium thiopental.).

Extraction

Following the shadow air drying, 500 g of powdered fruit peel was soaked in 2.5 L of methanol within a sealed amber-colored vessel for 15 days with irregular jerking. The resulting solvent mixture was filtered using a clean cotton pad and filter pad. The methanol was then removed using an “EYELA Rotavapor” rotary evaporator at lower pressures and approximately 40°C to yield 58 g of gummy extract from the methanolic extract of *C. reticulata* peel. This represented 11.6% of the weight of the powdered fruit peel.

Fractionation

Solvent-solvent differentiation of the extract was performed using S. Morris Kupchan's partitions (1970), as modified by VanWagenen et al.²² Five grams of crude extract were sequentially treated with water in methanol (1:9), petroleum ether (PESF), dichloromethane (DCMSF), ethyl acetate (EASF), and water (AQSF) to generate 4 distinct fractions. Each fraction was evaporated until completely dried. The yields for the petroleum ether, dichloromethane, ethyl acetate, and water-soluble fractions were 15%, 43%, 24%, and 18%, respectively.

Phytochemical isolation and detection through nuclear magnetic resonance (NMR) technique

Secondary metabolites were isolated from the methanolic crude extract, which was then subsequently purified using chromatographic techniques. The schematic flowchart of complete phytochemical extraction, fractionation, identification, and isolation of phytoconstituents from the *C. reticulata* is stated in supplementary Figure S2. The size exclusion chromatography used a gradient solvent system, with lipophilic sephadex LH 20 acting as the stationary phase. The ratios of the various solvents utilized as the mobile phase were as follows: n-hexane, dichloromethane (DCM), and methanol in a proportion of 2:5:1; 10% methanol in DCM; 50% methanol in DCM; and 100% methanol (supplementary Table S1). These fractions were thoroughly screened using thin-layer chromatography (TLC) on silica gel-coated metal plates (20 cm × 20 cm) with various solvent solutions. The obtained chromatogram was visually examined under UV illumination at 254 and 366 nm to identify fluorescence quenching. Colored compounds were also recognized after spraying the plate with a 1% vanillin-sulfuric acid solution and heating at 105°C for 2 to 3 minutes. Fractions with similar TLC patterns were combined, yielding 13 sub-fractions. The phytochemicals were then separated

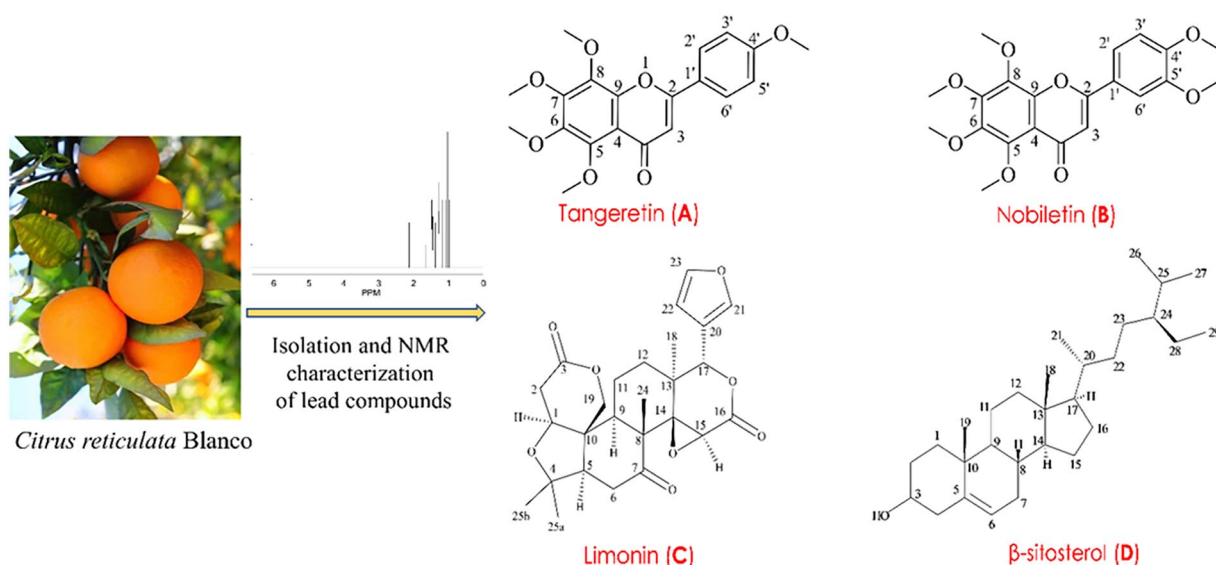


Figure 1. Structures of the identified and characterized compounds through the ^1H -NMR and chromatographic technique from the peel extract of *Citrus reticulata* Blanco.

and purified from these sub-fractions using repeated preparative thin layer chromatography (PTLC).

A total of 4 compounds (A-D; Figure 1) were isolated and characterized in the study through an extensive chromatographic and spectroscopic methods. Compound D was isolated from sub-fraction F-9 to F-12 (using a solvent mixture of 5% ethyl acetate in toluene), two compounds such as Compounds A (R_f -value=0.68) and B (R_f value=0.46) were isolated from sub-fraction F-23 to F-28 (using 5% methanol in chloroform). In addition, compound C was isolated from sub-fraction F-30 to F-34 (using 10% methanol in chloroform; R_f -value=0.55; Tables S2 and S3).

The total phytochemical isolation procedure and its schematic flowchart can be found in Supplemental Figure S2. Bruker AMX-400 NMR spectrometer was operated to generate ^1H -NMR spectra while all spectra were obtained in a deuterated chloroform solvent (CDCl_3). The peak values for chemical shift (δ) were standardized to tetramethylsilane (TMS) and the residual signals from the solvent.

GC-MS/MS analysis

The methanol extract of *C. reticulata* (MECR) was analyzed using the Shimadzu GC/MS-QP2010 ultra, which had an auto-sampler. A 5 MS/HP column (30 m, 0.25 mm, 0.25 m) was used, using pure helium as the mobile phase. The helium's linear speed was kept at 39 cm/s, with a circulation rate of 1.12 mL/min. The oven temperature raised at a rate of $10^\circ\text{C}/\text{min}$, ranging from 110°C to 280°C , while the needle temperature was set at 250°C . Injection volume of 50 μL was used in split-less mode with a 10:1 ratio. The detector voltage remained at 0.94 kV, while the ambient temperatures for the ion source, MS transfer line, and ion source were held at 200°C and 250°C , respectively. Full-scan mass spectra were obtained at 10 000 μs in the (m/z) range of 85 to 500. Peaks

and chemical ingredients were identified using a search of the National Institute of Standards and Technology (NIST) database.

Antimicrobial properties

A total of 13 various microbial species, encompassing 5 Gram-positive bacteria (*Bacillus subtilis*, *Bacillus megaterium*, *Bacillus cereus*, *Staphylococcus aureus*, and *Sarcina lutea*), 8 Gram-negative bacteria (*Salmonella typhi*, *Escherichia coli*, *Shigella boydii*, *Salmonella paratyphi*, *Shigella dysenteriae*, *Vibrio mimicus*, *Vibrio parahaemolyticus*, and *Pseudomonas aeruginosa*), along with 5 fungi (*Aspergillus niger*, *Candida albicans*, *Aspergillus fumigatus*, *Saccharomyces cerevisiae*, and *Aspergillus ustus*), were procured in their pure culture strains from the Bangladesh Council of Scientific and Industrial Research (BCSIR), Dhaka, Bangladesh.

The antibacterial efficacy of crude plant extracts and their various fractions was examined using the disk diffusion method.²³ In this process, 6 mm-diameter filter paper disks containing specified quantities of test samples (concentration of 400 $\mu\text{g}/\text{disk}$) were positioned on nutrient agar medium and uniformly inoculated with the respective microorganisms. These disks were then dried and sterilized. Antibiotics permeated the agar gel from a confined source, generating a concentration gradient. Ciprofloxacin standard antibiotic disks served as positive controls, while blank disks were utilized for the negative control. The petri dishes were refrigerated at a low temperature (4°C) for 16 to 24 hours to enhance the diffusion of test samples into adjacent media.²³ Following inversion and additional incubation at 37°C for 24 hours to promote optimal microbial growth around the disks was impeded by the test samples exhibiting antibacterial effects. This hindrance led to the formation of discernible zones of inhibition, and their

diameters were measured to assess the antibacterial activity of the test sample.^{23,24}

Anti-inflammatory effects

The crude methanolic extracts and fractions derived from the peel of *C. reticulata* were evaluated for *in vitro* anti-inflammatory activity by employing the established techniques as described by previous studies.^{23,25}

Hypotonic solution-induced anti-inflammatory effect. To evaluate the efficiency of MECR and its related extractives in stabilizing human erythrocyte membranes, we followed known techniques from a previous research.²⁵ Erythrocytes were extracted from a healthy adult weighing 70 kg with fair skin and stored in a sterile container with EDTA for anticoagulation. A buffer solution containing disodium phosphate and its conjugate acid, monosodium phosphate, was created to maintain a pH of 7.4. An isotonic solution (500 mL, 154 mM) was made by dissolving 4.5045 g of NaCl in sterile distilled water, whereas a hypotonic solution (500 mL, 50 mM) was made using 1.4625 g. The erythrocyte suspension was washed 3 times with buffer and isotonic solution before being centrifuged at 3000 rpm for 10 minutes. A stock RBC suspension (0.50 mL), a 10 mM sodium phosphate buffer (4.5 mL), a hypotonic solution (50 mM NaCl), and different quantities of extractives (2.0 mg/mL) or standard acetyl salicylic acid (ASA) (0.10 mg/mL) were used to create test samples. After a 10-minute incubation at room temperature, the solutions were centrifuged (3000 rpm for 10 minutes) and the supernatants' absorbance (optical density (OD)) was measured at 540 nm. The proportion of inhibition of hemolysis or stabilization of membrane was estimated by employing the formula stated below:

$$\begin{aligned} &\% \text{ inhibition of hemolysis (Hypotonic solution - induced)} \\ &= (\text{OD}_1 - \text{OD}_2) / \text{OD}_1 \times 100 \end{aligned}$$

Where, OD₁ and OD₂ represent the optical density of hypotonic buffered saline solution (control) and the investigated sample in hypotonic solution, respectively.

Heat-induced anti-inflammatory effect. Two sets of centrifuge tubes were created, each containing 5 mL of isotonic buffer, 1.0 mg/mL of methanolic peel extract, and different fractions. A control tube contained an equal volume of all substances except the test materials. In every well, 30 µL of erythrocyte suspension was added by inverse and gently stirring. One pair of tubes was placed in a 54°C water bath for 20 minutes, while the second set was maintained in a cold bath at 0°C to 5°C. After incubation, the supernatant was centrifuged (1300 rpm for 3 minutes), and the optical density (OD) was measured at 540 nm. The percentage inhibition of hemolysis in the investigations was estimated using the corresponding equation:

$$\begin{aligned} &\% \text{ hemolysis inhibition (Heat - induced)} \\ &= (1 - \text{OD}_2 - \text{OD}_1 / \text{OD}_3 - \text{OD}_1) \times 100 \end{aligned}$$

Where, OD₁, OD₂, and OD₃ refers to the optical density of the non-heated test sample, the heated test sample, and the heated control sample, respectively.

Thrombolytic properties

In vitro thrombolytic activity was determined using the blood clot lysis technique according to the methods described by Prasad et al.²⁶ The positive control was a lyophilized streptokinase vial containing 1 500 000 IU while the negative control was distilled water. Healthy volunteers' venous blood was collected in pre-weighed sterile micro-centrifuge tubes (1 mL/tube), then incubated at 37°C for 45 minutes. Following clot formation, the weight of each clot was determined after full serum extraction. Each micro-centrifuge tube with a pre-weighted clot received a 100 µL aqueous solution from different partitions, in addition to the crude extract. The tubes were incubated for 90 minutes at 37°C and kept in a close observation for clot lysis. The percentage of clot lysis was enumerated by using the following the formula:

$$\% \text{ of clot lysis} = (\text{Released clot weight} / \text{clot weight}) \times 100$$

Animal study design

The Animal Division of the International Centre for Diarrheal Diseases and Research in Bangladesh (ICDDR) provided Swiss albino adult mice aged 4 to 5 weeks and weighed 25 to 30 g. Prior to the animal research, these mice were kept in polypropylene cages under conventional climatic settings such as a 55% relative humidity level, 25°C ambient temperature, and a 12-hour light-dark cycle. Prior to the beginning of the experiments, the animals were allotted a week to acclimate to their new environment. During this time, the animals were fed a standard laboratory diet and had unlimited access to water. Their care and handling followed the guidelines set by the Swiss Academy of Medical Sciences (SAMS) and the Swiss Academy of Sciences. The study also complied with the latest Animal Research: Reporting of In Vivo Experiments (ARRIVE) guidelines.²⁷ The protocols for animal handling and procedures involved in the animal studies were thoroughly reviewed and approved by the Committee on Ethical Compliance in Research at the State University of Bangladesh, Dhaka, Bangladesh (approval number: 2022-01-23/SUB/A-ERC/006).

The study included 3 different doses of the methanol extract of *C. reticulata* (MECR) at concentrations of 100, 200, and 400 mg/kg body weight, designated as ME-100, ME-200, and ME-400, respectively. The animal subjects were divided into 5 groups, each consisting of 4 mice (n = 4). This sample size was estimated by using the "resource equation" method which was

clearly explained in the previous studies.²⁸⁻³⁰ The groupings were organized as follows:

- Group I (n=4): Normal saline water [0.9% (w/v) NaCl solution BP] as negative control
- Group II (n=4): Standard drug as positive control
- Group III (n=4): 100 mg/kg body weight MECR (ME-100)
- Group IV (n=4): 200 mg/kg body weight MECR (ME-200)
- Group V (n=4): 400 mg/kg body weight MECR (ME-400)

Central analgesic activity

The analgesic effects of MECR were assessed using a heat-based approach and the tail immersion experiment, as described by previous investigation.³¹ The positive control group received morphine (15 mg/mL) diluted with saline water to form the standard sample (subcutaneous, 2 mg/kg), as reported in earlier report.³² The mice received the test drugs orally using a feeding syringe. The experiment involves submerging a mouse's tail in water heated to 55°C. The Pain Response Time (PRT) or latency duration, which indicates how long it takes for each mouse to move its tail in hot water, was assessed at 0, 30, 60, and 90 minutes after the test samples were administered.

Peripheral analgesic activity

The peripheral analgesic effects of MECR were assessed by applying the acetic acid-induced writhing technique in mice model.³³ At the 0 hour of the experiment, the control group was administered normal saline, while the positive control group received diclofenac sodium (50 mg/kg) as standard. Subsequently, the 3 experimental groups were administered their respective doses of the designated crude extracts. After 60 minutes, all groups received an intraperitoneal injection of 1% glacial acetic acid (0.1 mL; dissolved in normal saline) to induce visceral pain. After 5 minutes of acetic acid injection, the writhing times were counted for 15 minutes. The formula for calculating the percentage of writhing inhibition was as follows:

$$\text{Percentage (\%)} \text{ of writhing inhibition} \\ = \left(\frac{N_{\text{Control}} - N_{\text{test}}}{N_{\text{Control}}} \right) \times 100\%$$

Where, N = average amount of stomach writhing for every group.

Anti-diarrheal activity

The anti-diarrheal activity of MECR was measured by employing a castor oil-induced diarrhea model in mice, outlined in

earlier studies.^{34,35} According to the experimental design, the positive control group received oral administration of loperamide (50 mg/kg bw). The weighted extracts, after being suspended with 1% Tween-80, were unidirectional handled and then applied to the test groups. The normal control group received only the normal saline water. To induce diarrhea, 1 mL of pure castor oil was supplied to each mouse after 1 hour. Each mouse was kept in a separate cage with blotting paper on the floor. For each test group, the floor lining of individual mouse cage was changed every hour. The number of diarrheal stools generated by each mouse was monitored hourly for up to 4 hours after castor oil delivery. The count of diarrheal feces produced by the mice was recorded at 1-hour intervals over a 4-hour observation period. The percentage inhibition of diarrheal episodes was subsequently calculated using the following equation.

$$\% \text{ inhibition of defecation} = \frac{D_{\text{control}} - D_{\text{test}}}{D_{\text{control}}} \times 100\%$$

Where, D = Average diarrheal episodes in every group.

Molecular docking

The isolated and purified 4 compounds (A-D) and 8 more compounds (C-79, C-83, C-84, C-86, C-87, C-88, C-90, and C-91) from the obtained compound list characterized by GC-MS/MS technique were chosen for a computational modeling study to predict their receptor binding profiles against the relevant target proteins to support the biological activities of the studied extracts and fractions. Following established procedures from several previous studies, molecular docking of these phytochemicals was conducted using BIOVIA Discovery Studio version 4.5, PyMOL 2.3, and PyRx software packages.³⁶⁻³⁹

Ligand preparation. A total of 12 phytochemicals were selected as ligands in docking investigation. These chemicals were identified as tangeretin (PubChem CID: 68077), nobiletin (PubChem CID: 72344), limonin (PubChem CID: 179651), β -sitosterol (PubChem CID: 481107734), salvigenin (PubChem CID: 161271), pentamethoxyflavone (PubChem CID: 35028119), 6-demoethoxytangeretin (PubChem CID: 629964), stigmasterol (PubChem CID: 5280794), pebrellin (PubChem CID: 632255), artemetin (PubChem CID: 5320351), senesetin (PubChem CID: 145659), dimethylnobiletin (PubChem CID: 358832) from PubChem database (retrieved on May 27, 2024). The standard drugs thrombolytic agent warfarin (PubChem CID: 54678486), cyclooxygenase inhibitor diclofenac (PubChem CID: 3033), antioxidant BHT (PubChem CID: 31404), antidiarrheal molecule loperamide (PubChem CID: 3955), antibacterial agent ciprofloxacin (PubChem CID: 2764) and μ -opioid receptor inhibitor morphine (PubChem CID: 5288826) were downloaded in SDF

format. Using the PubChem CIDs of the ligands, a ligand library in PDB format was created following the ligands' sequential loading into Discovery Studio version 4.5. Using the PM6 semi-empirical approach, the accuracy of molecular interactions for every ligand was enhanced.⁴⁰

Protein preparation. To predict the potential antibacterial, thrombolytic, anti-inflammatory, analgesic, and antidiarrheal activities of the ligands, a computational docking approach was employed. Specifically, dihydrofolate reductase (DHFR; PDB ID: 4M6J), tissue plasminogen activator (PDB ID: 1A5H), cyclooxygenase 2 (COX-2; PDB ID: 1CX2), μ -opioid receptor (MOR; PDB ID: 5C1M), and kappa opioid receptor (PDB ID: 6VI4) with their corresponding active sites were selected to assess antibacterial, thrombolytic, peripheral and central analgesic, and antidiarrheal effects, respectively, based on the previously published literature.^{23,41–43} In order to retrieve the target proteins, protein data bank was searched. After then, the three-dimensional (3D) crystal structures were downloaded and saved in PDB format (retrieved on May 27, 2024). Then the downloaded proteins were processed by using Discovery Studio (version 4.5) and Swiss PDB viewer for cleaning and optimizing purposes, respectively.⁴⁴

Protein and ligand interaction. The PyRx software was used for molecular interaction purpose. The cleaned and optimized proteins were imported in the software and selected as macromolecules. The active amino acids were assigned, which were pre-selected according to the literature data and summarized in the Supplemental Table S4. The 3D conformers of the ligands in SDF format were uploaded to the PyRx program and minimized energy using "uff force field." Then, all ligands were transformed into pdbqt format to determine the best hit. Then, as shown in Supplemental Table S4, the grid box was created, with the proteins' active binding sites centered inside. The other docking process parameters were kept at their factory default values. The final docked macromolecules and ligands were exported as pdbqt format output files, and the outcomes of the docking analysis were then investigated. PyMOL software was used to combine the stored ligands' output files and the macromolecule's pdbqt file in PDB format for further visualization. Discovery Studio Visualizer (version 4.5) was used for visualization and 2D figure development.

Pharmacokinetics and toxicity analysis. The pharmacokinetic parameters related to absorption, distribution, metabolism, excretion (ADME), and toxicity were predicted by employing the well-known online server pkCSM (<https://biosig.lab.uq.edu.au/pkcsm/prediction>; accessed on May 10, 2024).

Physicochemical and drug-likeness analysis. All the docked 12 compounds were assessed for their potential drug-like properties according to Lipinski's rule of 5 (molar refractivity between

40 and 130, molecular weight ≤ 500 ; H-bond acceptors < 10 ; H-bond donors < 5 ; and LogP ≤ 5) using the Swiss ADME online tool (www.swissadme.ch; accessed on May 27, 2024).

Statistical analysis

The data processing and findings interpretation were done in accordance with the established protocols explained by Assel et al.⁴⁵ The *in vitro* experimental analysis, graphs and data processing were carried out using Microsoft Excel (version 10.0). Additionally, the treated groups were compared to the control (vehicle) group in order to do the statistical analysis for the *in vivo* experiments. The mean values, along with their corresponding standard errors of mean (SEM), were represented as mean \pm SEM to indicate the outcomes of the *in vivo* assessments. The results from *in vivo* testing were examined and analyzed through GraphPad Prism software (version 8.0.2). A one-way ANOVA was conducted on all variables, followed by Student's *t*-test. *P*-values less than .05 were considered statistically significant. The heatmap representing the docking score analysis and the graphs associated with the *in vivo* studies were generated utilizing GraphPad Prism software.

Results

Phytochemical studies

Four compounds were identified, purified, and characterized during the phytochemical isolation process through various chromatographic techniques and ¹H-NMR spectroscopic analysis. These compounds were determined to be tangeretin (compound A), nobiletin (compound B), limonin (compound C), and β -sitosterol (compound D). Additionally, 91 compounds were detected and characterized using GC-MS/MS analysis. Further detailed information is provided in the following sections.

Compounds characterization by NMR technique

Compound A: According to the ¹H-NMR spectrum and the summarized data in Table 1, the presence of 5 singlets at δ 3.88, 3.94, 3.96, 4.01, and 4.09 ppm indicated the existence of 15 protons of 5 methoxy groups. Additionally, a singlet at δ 6.60 ppm suggested that compound A have an olefinic proton, a key feature of flavone-type molecules. The presence of 2 doublets at δ 7.15 and 7.85 ppm, with a coupling constant of nearly 8.0 Hz, indicates a 1,4-substituted benzene ring within compound A. Moreover, matching this ¹H-NMR spectrum with the existing literature suggested the identification compound A as tangeretin.⁴⁶

Compound B: The double doublets at δ 7.56 ppm, doublet at δ 6.88 ppm, and another doublet at δ 7.40 ppm denoted the presence of 1, 3, 4 tri-substituted benzene ring of the compound B. The appearance of 6 singlets at δ 4.9, 4.03,

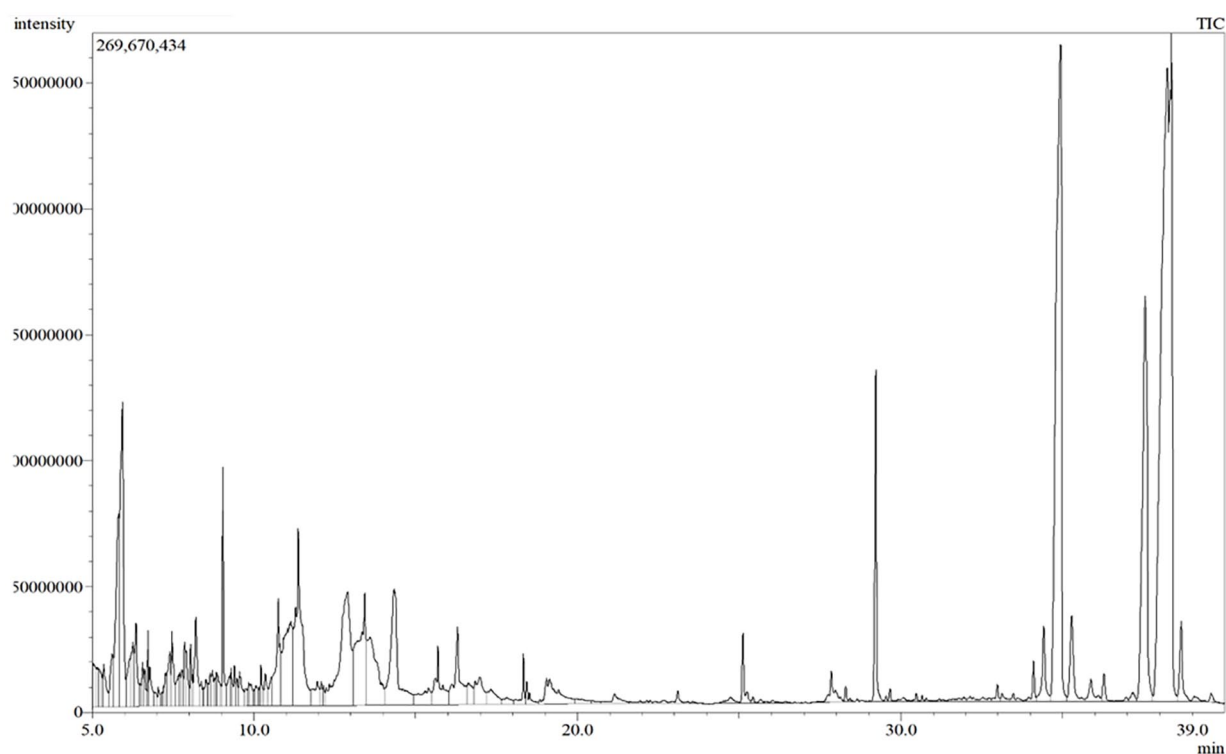


Figure 2. GC-MS spectrum of the crude extract obtained from *Citrus reticulata* Blanco.

4.01, 3.97, 3.95, and 3.94 ppm showed the presence of 6 difference methoxy groups within the compound B. In addition, the singlet at δ 6.61 ppm represents 1 olefinic proton. This ^1H -NMR spectrum values indicated this molecule might be a polymethoxyflavone containing total 6 methoxy groups. After that, matching the proton NMR values with the previously published literature suggested this molecule as nobiletin.⁴⁷

Compound C: According to the ^1H -NMR spectrum and the Table 1, the presence of a multiplet at δ 7.40 and δ 6.49 indicated a furan ring within this molecule. Moreover, 3 different singlets at δ 1.08 (3H), δ 1.17 (6H), and δ 1.28 (3H) suggested the existence of 4 branched methyl groups within the molecule. A multiplet at δ 3.98 showed that C-1 was attached to a highly electronegative group. Furthermore, a singlet at δ 4.04 demonstrated that H-15 was attached to an oxygenated carbon moiety. Another singlet at δ 5.46 showed that H-17 was linked to the furan group of this molecule. Two doublets at δ 4.75 ($J=12.8\text{ Hz}$) and δ 4.45 ($J=13.2\text{ Hz}$) indicated that both protons of H-19 were connected to an oxygenated carbon moiety. Additionally, various broad doublet (br. d) peaks within the δ 2.21 to δ 2.97 range indicated several protons in the molecule's skeleton, such as H-2a, H-2b, H-6a, H-6b, H-5, and H-9. This data aligns with previously published proton NMR data in the literature, supporting the conclusion that the compound is limonin.⁴⁸

Compound D: The presence of multiplet at δ 5.34 ppm suggested the presence of steroidal olefinic proton at H-6

position. While multiplet at δ 3.58 ppm recommended the H-3 is attached with the highly electro negative moiety. Furthermore, the presence of 2 singlets, 3 doublets, and 1 triplet peaks ranging from 0.67 to 0.99 ppm demonstrated the presence of 6 steroidal methyl groups within the compound D. In addition, by matching the ^1H -NMR spectrum of the compound D with the literature ^1H -NMR values, it was confirmed as β -sitosterol.⁴⁹

Compounds detection by GC-MS analysis

A total of 91 phytoconstituents were predominantly detected in the MECR through GC-MS technique. The spectrum obtained from the GC-MS/MS analysis is available in Figure 2. Among the identified over 90 compounds, a significant number of compounds were polymethoxyflavones. Among these, the following were quantified: nobiletin (29.04%), tangeretin (15.55%), artemetin (8.1%), 6-demethoxytangeretin (1.28%), sinensetin (0.95%), demethylnobiletin (0.14%), pebrellin (0.10%), and salvigenin (0.04%). Furthermore, some notable compounds were also detected as dihydrocarvyl acetate (4.07%), Methyl alpha D-galactopyranoside (3.37%), 3',5'-demethoxy-acetaophenone (2.55%), D-limonene (2.48%), and stigmaterol (0.35%; Table 2). Yet, some phytoconstituents were discovered as least amount such as β -Elemene, Megastigmatrienone, Octadecanamide, Fenoterol, Salvigenin, and Bicyclon onan-2-one, 8-isopropylidene- (0.04%). Various classes of phytoconstituents such as fatty derivatives (Methyl 3-hydroxydodecanoate, 2,6,9,11-Dodecatetraenal, 2,6,10-trimethyl-, (*E,E,E*)-, and Hexane,1- (isopropylidene cyclopropyl)-,) steroids

Table 1. The ¹H-NMR (400 MHz, CD₃OD) and the compared literature spectroscopic data of the isolated compounds A–D from *C. reticulata*.

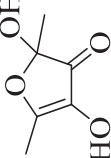
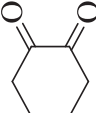
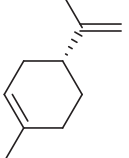
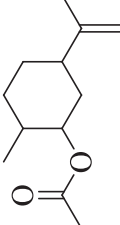
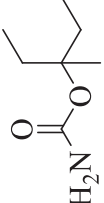
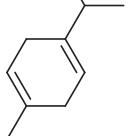
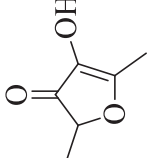
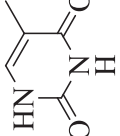
COMPOUNDS	MOL. FORMULA	MOL. WT. (G/MOL)	POSITIONS	¹ H-NMR VALUES δ IN PPM (400MHZ, CDCL ₃)	REFERENCE VALUES	REF.
Tangeretin (A)	C ₂₀ H ₂₀ O ₇	372.4	H-3	6.60 (1H, s)	6.69 (1H, s)	Morimoto et al ⁴⁶
			H-2'/H-6'	7.85 (2H, d, J=8Hz)	7.96 (2H, d, J=9.0Hz)	
			H-3'/H-5'	7.15 (2H, d, J=8.4Hz)	7.10 (2H, d, J=9.0Hz)	
			5 Methoxy groups	(3.88, 3.94, 3.96, 4.01, 4.09 (Total five s, 15H)	3.97, 4.03, 4.06, 4.10, 4.18 (Total five s, 15H)	
Nobiletin (B)	C ₂₁ H ₂₂ O ₈	402.4	H-3	6.61 (1H, s)	6.63 (1H, s)	Santos et al ⁴⁷
			H-2'	7.56 (1H, dd, J=8.4, 2.0Hz)	7.47 (1H, dd, J=8.5, 2.1 Hz)	
			H-3'	6.98 (1H, d, J=8.8Hz)	6.99 (1H, d, J=8.5Hz)	
			H-6'	7.40 (1H, d, J=2Hz)	7.42 (1H, d, J=2.1Hz)	
			6 Methoxy groups	4.9, 4.03, 4.01, 3.97, 3.95, 3.94, (Total six s, 18H)	4.10, 3.95, 3.95, 4.03, 3.98, 3.96 (Total six s, 18H)	
Limonin (C)	C ₂₆ H ₃₀ O ₈	470.5	H-1	3.98 (1H, m)	4.03 (1H, m)	Brekša et al ⁴⁸
			H-2a	2.66 (1H, br. d, J=16.8Hz)	2.67 (1H, dd, J=16.8, 2.0Hz)	
			H-2b	2.97 (1H, br. d, J=16.8Hz)	2.98 (1H, dd, J=16.8, 4.0Hz)	
			H-3	-	-	
			H-4	-	-	
			H-5	2.21 (1H, br. d, J=15.2Hz)	2.22 (1H, dd, J=15.8, 3.4Hz)	
			H-6a	2.42 (1H, br. d, J=14.8Hz)	2.46 (1H, dd, J=14.4, 3.2Hz)	
			H-6b	2.86 (1H, br. d, J=14.8Hz)	2.85 (1H, dd, J=15.8, 14.6Hz)	
			H-7	-	-	
			H-8	-	-	
			H-9	2.53 (1H, br. d, J=11.6Hz)	2.55 (1H, dd, J=12.2, 3.0Hz)	
			H-11	1.76-1.88 (2H, m)	1.72-1.95 (2H, m)	
			H-12	1.36-1.46 (2H, m)	1.46-1.58 (2H, m)	
			H-14	-	-	

(Continued)

Table 1. (Continued)

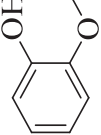
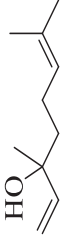
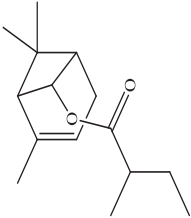
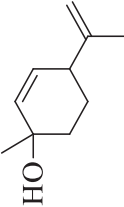

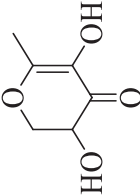

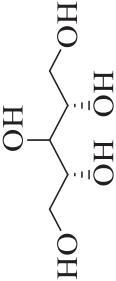
COMPOUNDS	MOL. FORMULA	MOL. WT. (G/MOL)	POSITIONS	¹ H-NMR VALUES δ IN PPM (400MHZ. CDCL ₃)	REFERENCE VALUES	REF.
β-sitosterol (D)	C ₂₉ H ₅₀ O	414.7	H-15	4.04 (1H, s)	4.05 (1H, s)	Majid Shah et al ⁴⁹
			H-16	-	-	
			H-17	5.46 (1H, s)	5.47 (1H, s)	
			H-18, H-25b	1.17 (6H, s)	1.18 (6H, s)	
			H-19a	4.75 (1H, d, J= 12.8Hz)	4.76 (1H, d, J= 13.0Hz)	
			H-19b	4.45 (1H, d, J= 13.2 Hz)	4.46 (1H, d, J= 13.0Hz)	
			H-20	-	-	
			H-21, H-23	7.39-7.40 (2H, m)	7.40-7.41 (2H, m)	
			H-22	6.49 (1H, m)	6.34 (1H, m)	
			H-24	1.08 (3H, s)	1.08 (3H, s)	
			H-25a	1.28 (3H, s)	1.29 (3H, s)	
			H-3	3.58 (1H, m)	3.53 (1H, tdd)	
			H-6	5.34 (1H, m)	5.36 (1H, t, J=6.4Hz)	
			H-18	0.67 (3H, s)	0.68 (3H, s)	
			H-19	0.99 (3H, s)	1.01 (3H, s)	
			H-21	0.91 (3H, d, J=6.8Hz)	0.93 (3H, d, J=6.5Hz)	
			H-26	0.80 (3H, d, J=8.4Hz)	0.81 (3H, d, J=6.4 Hz)	
			H-27	0.84 (3H, d, J=7.6 Hz)	0.83 (3H, d, J=6.4 Hz)	
			H-29	0.87 (3H, t, J=6.0Hz)	0.84 (3H, t, J=7.2Hz)	

Table 2. The identified and characterized phytoconstituents obtained from GC-MS/MS analysis are presented with details including the compound names, retention time (RT), percentage of area, molecular weight (g/mol), molecular formula, PubChem CID, and their chemical structures drawn using ChemDraw. Additionally, the pharmacological activities of these compounds were extracted from the literature, with the corresponding references cited in the final column.

SL NO.	COMPOUND	RT (MIN)	AREA %	MOL. WEIGHT (G/MOL)	MOLECULAR FORMULA	PUBCHEM	CHEMICAL STRUCTURE	PHARMACOLOGICAL ACTIVITY	REF
1.	2,4-Dihydroxy-2,5-Dimethyl-3(2H)-furan-3-one	5.36	0.1	144.12	C ₆ H ₈ O ₄	538757		Antioxidant activity	Chukwu et al ⁵⁰
2.	1,2-Cyclohexanedione	5.62	0.45	112.13	C ₆ H ₈ O ₂	13006		N/A	
3.	D-Limonene	5.82	2.48	136.23	C ₁₀ H ₁₆	440917		Antioxidant, antidiabetic, anticancer	Anandakumar et al ⁵¹
4.	Dihydrocarvyl acetate	5.935	4.07	196.29	C ₁₂ H ₂₀ O ₂	30248		Antimicrobial, antioxidant, insecticidal, antitumor, anti-inflammatory and antidiabetic	Zhang et al ⁵²
5.	Emylcanate	6.145	0.47	145.2	C ₇ H ₁₅ NO ₂	6526		Antioxidant and anticancer	Onyegeme-Okerenta et al ⁵³
6.	Gamma-Terpinene	6.264	0.6	136.23	C ₁₀ H ₁₆	7461		Antimicrobial, antioxidant, hypoglycemic, hypolipidemic, anxiolytic, analgesic, anti-inflammatory, anti-convulsant and anticancer	Laribi et al ⁵⁴
7.	Furaneol	6.363	0.76	128.13	C ₆ H ₈ O ₃	19309		Antimicrobial activity	Sung et al ⁵⁵
8.	Thymine	6.565	0.3	126.11	C ₅ H ₈ N ₂ O ₂	1135		Antibacterial activity	Liu et al ⁵⁶

(Continued)

Table 2. (Continued)

SL NO.	COMPOUND	RT (MIN)	AREA %	MOL. WEIGHT (G/MOL)	MOLECULAR FORMULA	PUBCHEM	CHEMICAL STRUCTURE	PHARMACOLOGICAL ACTIVITY	REF
9.	Phenol, 2-methoxy-	6.616	0.2	124.14	C ₇ H ₈ O ₂	460		Antioxidant	Fujisawa et al ⁵⁷
10.	Linalool	6.728	0.23	154.25	C ₁₀ H ₁₈ O	6549		Antimicrobial, antioxidant, hypoglycemic, hypolipidemic, anxiolytic, analgesic, anti-inflammatory, anti-convulsant and anti-cancer.	Laribi et al ⁵⁴
11.	Chrysantenyl 2-methylbutanoate	7.05	0.06	236.35	C ₁₉ H ₂₄ O ₂	91693263		Antioxidant and anticancer	Ambati et al ⁵⁸
12.	2-Cyclohexen-1-ol,1-methyl-4-(1-methylethenyl)-,trans-	7.21	0.1	152.23	C ₁₀ H ₁₆ O	155626		Antibacterial and antifungal activity	Mehani et al ⁵⁹
13.	Ethanimine,N-ethyl-N-nitroso-	7.275	0.16	102.14	C ₄ H ₁₀ N ₂ O	5921		N/A	
14.	4H-Pyran-4-one,2,3-dihydro-3,5-dihydroxy-6-methyl-	7.403	0.55	144.12	C ₆ H ₈ O ₄	119838		Antioxidant activity	Chen et al ⁶⁰
15.	Trimethylene borate	7.47	0.5	243.9	C ₉ H ₁₈ B ₂ O ₆	88725		Antimicrobial activity	Zamakshshari et al ⁶¹
16.	Ribitol	7.615	0.15	152.15	C ₅ H ₁₂ O ₅	6912		Anti-diabetic	Montague and Taylor ⁶²

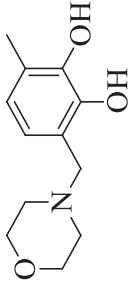
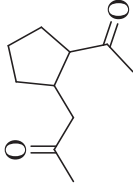
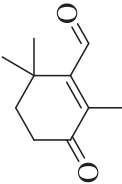
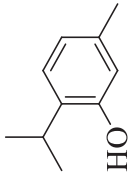
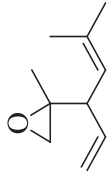
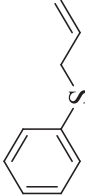
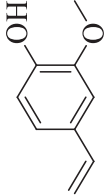

(Continued)

Table 2. (Continued)

SL NO.	COMPOUND	RT (MIN)	AREA %	MOL. WEIGHT (G/MOL)	MOLECULAR FORMULA	PUBCHEM	CHEMICAL STRUCTURE	PHARMACOLOGICAL ACTIVITY	REF
17.	Terpinen-4-ol	7.709	0.2	154.25	C ₁₀ H ₁₈ O	11230		Antimicrobial activity	Mondello et al ⁶³
18.	Bicyclo[2.2.2]octane-1,4-diol	7.779	0.25	142.2	C ₈ H ₁₄ O ₂	559236		N/A	
19.	alpha-Terpineol	7.859	0.35	154.25	C ₁₀ H ₁₈ O	17100		Antioxidant, anticancer, anticonvulsant, antitumor, antihypertensive, antinociceptive	Khaleel et al ⁶⁴
20.	8-Azabicyclo[3.2.0]hept-6-en-3-one, 8-methyl-	7.915	0.36	137.18	C ₈ H ₁₁ NO	565060		N/A	
21.	5-Methylbenzofuran-2,3-dione	8.048	0.23	162.14	C ₉ H ₆ O ₃	56974146		Anti-inflammatory, antimicrobial, antifungal, antihyperglycemic, analgesic, antiparasitic, and antitumor activities	Khodarahmi et al ⁶⁵
22.	Hexane,1-(isopropylidene)cyclopropyl)-	8.1	0.09	166.3	C ₁₂ H ₂₂	32479		Antioxidant activity	Erwin et al ⁶⁶
23.	5-(Hydroxymethyl)furfural	8.208	0.84	126.11	C ₆ H ₆ O ₃	237332		Antioxidant antitumor anti-inflammatory	Zhao et al ⁶⁷
24.	(-)-Carvone	8.376	0.11	150.22	C ₁₀ H ₁₄ O	439570		Antidiabetic, anti-inflammatory, anticancer, neurological, antimicrobial, antiparasitic, antiarthritic, anticonvulsant, and immunomodulatory effects.	Bouyahya et al ⁶⁸

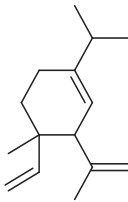

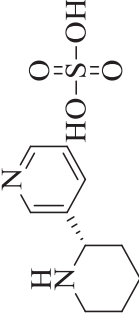
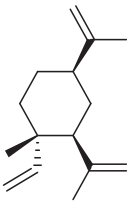
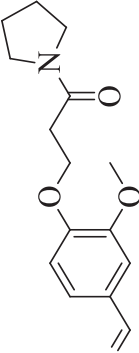
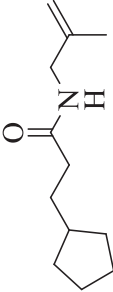
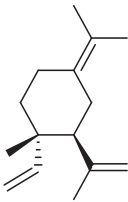
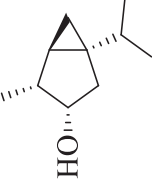
(Continued)

Table 2. (Continued)

SL NO.	COMPOUND	RT (MIN)	AREA %	MOL. WEIGHT (G/MOL)	MOLECULAR FORMULA	PUBCHEM	CHEMICAL STRUCTURE	PHARMACOLOGICAL ACTIVITY	REF
25.	1,2-Benzenediol, 3-methyl-6-(4-morpholinylmethyl)-	8.52	0.26	223.27	C ₁₂ H ₁₇ NO ₃	11333553		Antimicrobial activity	Naksing et al ⁶⁹
26.	1-Acetyl-2-(2'-oxo-propyl)-cyclopentane	8.651	0.12	168.23	C ₁₀ H ₁₆ O ₂	538127		N/A	
27.	β-Cyclocitral	8.724	0.21	166.22	C ₁₀ H ₁₄ O ₂	642490		Antifungal, anticancer, antimicrobial, and antiplasmodial	Faizan et al ⁷⁰
28.	Thymol	8.785	0.09	150.22	C ₁₀ H ₁₄ O	6989		Antioxidant, anti-inflammatory, antiseptic, and antibacterial and antifungal	Marchese et al ⁷¹
29.	Santolina epoxide	8.849	0.13	152.23	C ₁₀ H ₁₆ O	565371		N/A	
30.	Allylphenyl sulfide	8.895	0.17	150.24	C ₉ H ₁₀ S	79180		N/A	
31.	2-Methoxy-4-vinylphenol	9.048	1.1	150.17	C ₉ H ₁₀ O ₂	332		Anti-proliferative anti-inflammatory anticancer activity	Jeong and Jeong ⁷²
32.	Phytol	9.25	0.22	296.5	C ₂₀ H ₄₀ O	5280435		Anxiolytic, cytotoxic, antioxidant, anti-inflammatory, antimicrobial activity.	Islam et al ⁷³

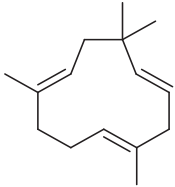
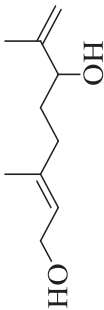
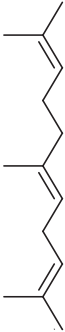

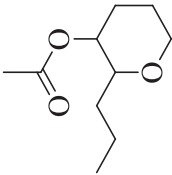
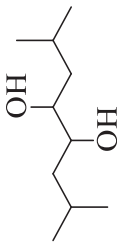

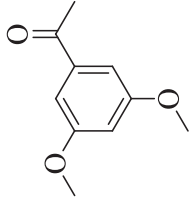
(Continued)

Table 2. (Continued)

SL NO.	COMPOUND	RT (MIN)	AREA %	MOL. WEIGHT (G/MOL)	MOLECULAR FORMULA	PUBCHEM	CHEMICAL STRUCTURE	PHARMACOLOGICAL ACTIVITY	REF
33.	delta-Elementene	9.3	0.14	204.35	C ₁₅ H ₂₄	89316		N/A	
34.	Decanal dimethyl acetal	9.557	0.19	202.33	C ₁₂ H ₂₆ O ₂	24513		N/A	
35.	3-(2-(piperidinyl) sulfate	9.735	0.06	260.31	C ₁₀ H ₁₆ N ₂ O ₄ S	205585		N/A	
36.	β-Elementene	9.843	0.04	204.35	C ₁₅ H ₂₄	6918391		Anti-inflammatory and antitumor	Shamsizadeh et al ⁷⁴
37.	3-Methoxy-4-(3-oxo-3-(pyrrolidin-1-yl)propoxy)benzaldehyde	9.93	0.09	277.31	C ₁₅ H ₁₉ NO ₄	91721113		N/A	
38.	3-Cyclopentylpropionamide, N-methyl-	10.06	0.10	195.3	C ₁₂ H ₂₁ NO	91695995		N/A	
39.	Gamma-elementene	10.219	0.12	204.35	C ₁₅ H ₂₄	6432312		N/A	
40.	Alpha-Thujone	10.355	0.17	154.25	C ₁₀ H ₁₈ O	12304610		5-HT3 receptor antagonist	Tamer et al ⁷⁵

(Continued)

Table 2. (Continued)

SL NO.	COMPOUND	RT (MIN)	AREA %	MOL. WEIGHT (G/MOL)	MOLECULAR FORMULA	PUBCHEM	CHEMICAL STRUCTURE	PHARMACOLOGICAL ACTIVITY	REF
41.	Humulene	10.54	0.32	204.35	C ₁₅ H ₂₄	5281520		Antioxidant, anticancer	Russo and Marcu ⁷⁶
42.	(2E)-3,7-dimethylocta-2,7-diene-1,6-diol	10.761	0.82	170.25	C ₁₀ H ₁₈ O ₂	12536844		Antimicrobial activity	
43.	Alpha-Farnesene	10.80S	0.24	204.35	C ₁₅ H ₂₄	5281516		Anti-viral	Habibah et al ⁷⁷
44.	Cis-5-Dodecenoic acid, methyl ester	10.915	0.51	212.33	C ₁₃ H ₂₄ O ₂	14524604		N/A	
45.	Acetic acid, 2-propyltetrahydropyran-3-yl ester	10.96	0.62	186.25	C ₁₀ H ₁₈ O ₃	537808		N/A	
46.	4,5-Octanediol, 2,7-dimethyl-	11.14	1.21	174.28	C ₁₀ H ₂₂ O ₂	549801		N/A	
47.	Dodecanoic acid	11.29	0.92	200.32	C ₁₂ H ₂₄ O ₂	3893		N/A	
48.	3',5'-Dimethoxyacetophenone	11.376	2.55	180.2	C ₁₀ H ₁₂ O ₃	95997		N/A	

(Continued)

Table 2. (Continued)

SL NO.	COMPOUND	RT (MIN)	AREA %	MOL. WEIGHT (G/MOL)	MOLECULAR FORMULA	PUBCHEM	CHEMICAL STRUCTURE	PHARMACOLOGICAL ACTIVITY	REF
49.	Megastigmatrienone	12.089	0.04	190.28	C ₁₃ H ₁₈ O	5375190		N/A	
50.	Isovaleric acid, eicosyl ester	12.48	0.11	382.7	C ₂₅ H ₅₀ O ₂	85768020		N/A	
51.	Methyl alpha D-Galactopyranoside	12.901	3.37	194.18	C ₇ H ₁₄ O ₆	76935		N/A	
52.	Methyl 3-hydroxydodecanoate	13.18	1.36	230.34	C ₁₃ H ₂₆ O ₃	155752		N/A	
53.	2,6,9,11-Dodecatetraenal, 2,6,10-trimethyl-, (E,E,E)-	13.424	1.39	218.33	C ₁₅ H ₂₂ O	5281534		N/A	
54.	2,3-Anhydro-d-mannosan	14.336	2.25	144.12	C ₆ H ₈ O ₄	88413508		N/A	
55.	Ethyl 2,2-dimethyl-5-oxoheptanoate	15.59	0.16	200.27	C ₁₁ H ₂₀ O ₃	545903		N/A	
56.	Penicillin Roquefort Toxin	15.845	0.06	320.3	C ₁₇ H ₂₀ O ₆	440907		Antimicrobial, genotoxic and cytotoxic	Dubey et al ⁷⁸
57.	dl-Citrulline	16.11	0.14	175.19	C ₆ H ₁₃ N ₃ O ₃	833		N/A	

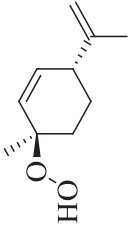

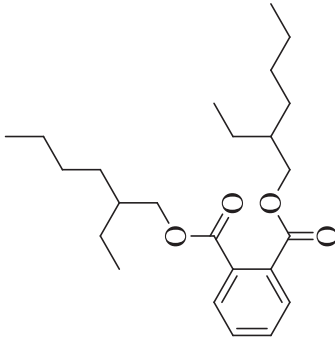
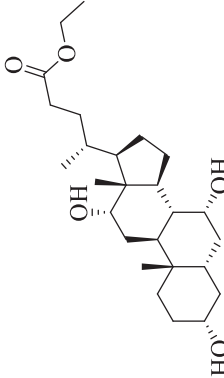
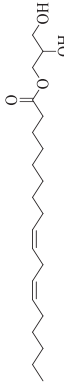



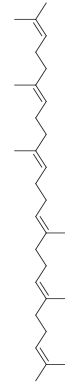
(Continued)

Table 2. (Continued)

SL NO.	COMPOUND	RT (MIN)	AREA %	MOL. WEIGHT (G/MOL)	MOLECULAR FORMULA	PUBCHEM	CHEMICAL STRUCTURE	PHARMACOLOGICAL ACTIVITY	REF
58.	n-Hexadecanoic acid	16.295	0.79	256.42	C ₁₆ H ₃₂ O ₂	985		Antioxidant, anti-inflammatory, antibacterial, antifungal	Mazumder et al ⁷⁹
59.	Scoparone	16.63	0.24	206.19	C ₁₁ H ₁₀ O ₄	8417		N/A	
60.	trans-Shinapyl alcohol	16.845	0.11	210.23	C ₁₁ H ₁₄ O ₄	5280507		Anti-inflammatory	Choi et al ⁸⁰
61.	Trehalose	16.987	0.26	342.3	C ₁₂ H ₂₂ O ₁₁	7427		Anti-inflammatory, anti-cancer	Frapporti et al ⁸¹
62.	Methyl 10- trans,12- cis-octadecadienoate	18.334	0.26	294.5	C ₁₉ H ₃₄ O ₂	5471014		N/A	
63.	91215-O ctadecatrienoic acid, methyl ester, (Z,Z,Z)-	18.434	0.1	292.5	C ₁₉ H ₃₂ O ₂	9316		Anti-cancer	Al-Otaibi et al ⁸²
64.	Linoleic acid trimethylsilyl ester	19.05	0.23	352.6	C ₂₁ H ₄₀ O ₂ Si	5352430		Antimicrobial activity, antibacterial activity	Rossellia et al ⁸³
65.	91215-O ctadecatrienoic acid,(Z,Z,Z)-	19.141	0.43	278.4	C ₁₈ H ₃₀ O ₂	5280934		Antibacterial, anti-inflammatory	Al-Otaibi et al ⁸²
66.	E,E,Z-1,3,12-Nonadecatriene-5,14-diol	19.43	0.12	294.5	C ₁₉ H ₃₄ O ₂	5364768		N/A	
67.	Benzyl Beta-D-Glucopyranoside	21.149	0.08	270.28	C ₁₉ H ₁₈ O ₆	188977		N/A	

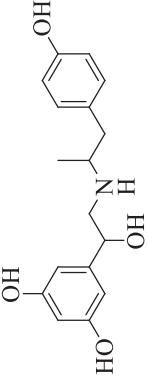
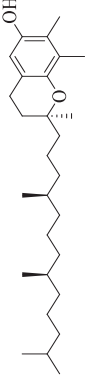
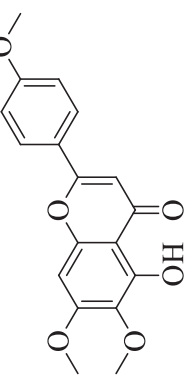
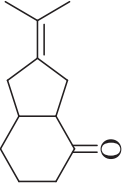
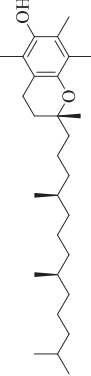
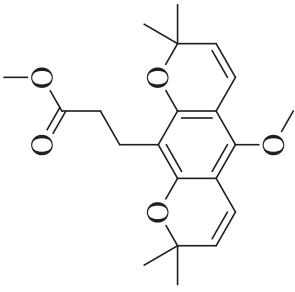
(Continued)

Table 2. (Continued)

SL NO.	COMPOUND	RT (MIN)	AREA %	MOL. WEIGHT (G/MOL)	MOLECULAR FORMULA	PUBCHEM	CHEMICAL STRUCTURE	PHARMACOLOGICAL ACTIVITY	REF
68.	(3R,6R)-3-Hydroperoxy-3-methyl-6-(prop-1-en-2-yl) cyclohex-1-ene	23.101	0.11	168.23	C ₁₀ H ₁₆ O ₂	6431185		N/A	
69.	Hexadecanoic acid 2-hydroxy-1-(hydroxymethyl) ethyl ester	25.119	0.48	330.5	C ₁₉ H ₃₈ O ₄	129853056		Antioxidant, anti-inflammatory and anthelmintic activities	Ali et al ⁸⁴
70.	Bis(2-ethylhexyl) phthalate	25.44	0.05	390.6	C ₂₄ H ₃₈ O ₄	8343		Antimicrobial activity	Habib and Karim ⁸⁵
71.	Ethyl Cholate	27.73	0.08	436.6	C ₂₆ H ₄₄ O ₅	6452096		N/A	
72.	Glycerol monolinoleate	27.85	0.27	354.5	C ₂₁ H ₃₈ O ₄	5283469		N/A	
73.	cis,cis,cis-7,10,13-Hexadecatrienal	28	0.14	234.38	C ₁₆ H ₂₆ O	5367366		N/A	
74.	cis-11-Eicosenamide	29.228	2.64	309.5	C ₂₀ H ₃₈ NO	5365374		N/A	
75.	Octadecanamide	29.539	0.04	283.5	C ₁₈ H ₃₇ NO	31292		N/A	
76.	Squalene	29.663	0.08	410.7	C ₃₀ H ₅₀	638072		Anticancer, antioxidant,	Kim and Karadeniz ⁸⁶

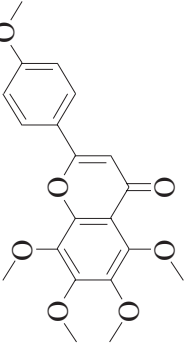
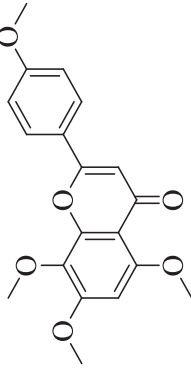
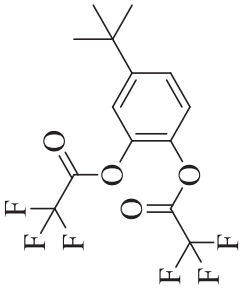
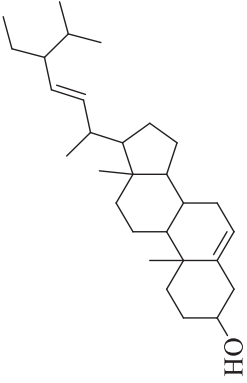
(Continued)

Table 2. (Continued)

SL NO.	COMPOUND	RT (MIN)	AREA %	MOL. WEIGHT (G/MOL)	MOLECULAR FORMULA	PUBCHEM	CHEMICAL STRUCTURE	PHARMACOLOGICAL ACTIVITY	REF
77.	Fenoterol	30.481	0.04	303.35	C ₁₇ H ₂₁ NO ₄	3343		Antibacterial	Soliman et al ⁸⁷
78.	Gamma-Tocopherol	32.979	0.1	416.7	C ₂₈ H ₄₈ O ₂	10740654		Antioxidant	Sánchez-Illana et al ⁸⁸
79.	Salvigenin	33.128	0.04	328.3	C ₁₈ H ₁₆ O ₆	161271		Anti-inflammatory, anti-cancer	Mansourabadi et al ⁸⁹
80.	Bicyclo[4.3.0]nonan-2-one, 8-isopropylidene-	33.469	0.04	178.27	C ₁₂ H ₁₈ O	596085		N/A	
81.	Vitamin E	34.099	0.28	430.7	C ₂₃ H ₅₀ O	14985		Antioxidant anti-inflammatory	Sánchez-Illana et al ⁸⁸
82.	Methylerlstoate	34.41.8	0.95	358.4	C ₂₁ H ₂₆ O ₅	631241		N/A	

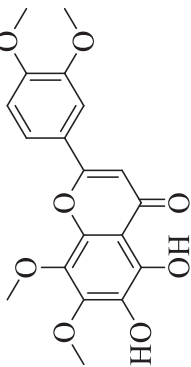
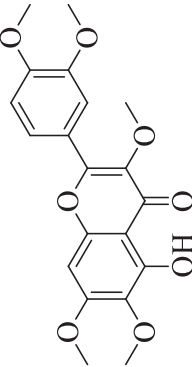
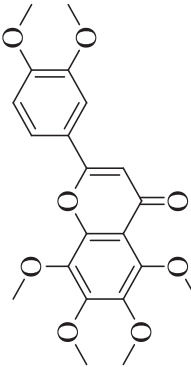
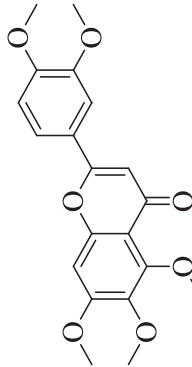
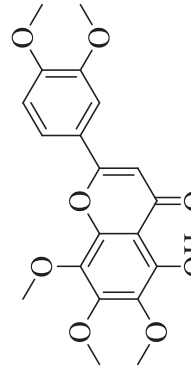
(Continued)

Table 2. (Continued)

SL NO.	COMPOUND	RT (MIN)	AREA %	MOL. WEIGHT (G/MOL)	MOLECULAR FORMULA	PUBCHEM	CHEMICAL STRUCTURE	PHARMACOLOGICAL ACTIVITY	REF
83.	Tangeretin (Compound A)	34.934	15.55	372.4	C ₂₀ H ₂₀ O ₇	35028119		Anti-inflammatory, anti-proliferative and neuroprotective	Hung et al ⁹⁰
84.	6-Demethoxytangeretin	35.283	1.28	342.3	C ₁₉ H ₁₈ O ₆	629964		Anti-inflammatory, anti-cancer	Li et al ⁹¹
85.	4-tert-Butylcatechol, bis(trifluoroacetate)	35.871	0.38	358.23	C ₁₄ H ₁₂ F ₆ O ₄	91743313		Antioxidant	Garcia-Moreno et al ⁹²
86.	Stigmasterol	36.272	0.35	412.7	C ₂₈ H ₄₈ O	5280794		Antimicrobial, anticancer, diuretic, anti-inflammatory, antioxidant	Hossain et al ⁹³

(Continued)

Table 2. (Continued)

SL NO.	COMPOUND	RT (MIN)	AREA %	MOL. WEIGHT (G/MOL)	MOLECULAR FORMULA	PUBCHEM	CHEMICAL STRUCTURE	PHARMACOLOGICAL ACTIVITY	REF
87.	Pebrellin	37.167	0.1	374.3	C ₁₉ H ₁₈ O ₈	632255		Antibacterial	Mamadallewa et al ⁹⁴
88.	Artemetin	37.546	8.1	388.4	C ₂₀ H ₂₀ O ₈	5320351		Anti-edematogenic activity	Bayeux et al ⁹⁵
89.	Nobiletin (Compound B)	38.359	29.04	402.4	C ₂₁ H ₂₂ O ₈	72344		Antioxidant, anticancer, anti-inflammatory, anti-tumor	Li et al ⁹¹
90.	Sinensetin	38.661	0.95	372.4	C ₂₀ H ₂₀ O ₇	145659		Anticancer, anti-inflammatory, antioxidant, antimicrobial, anti-obesity, anti-dementia	Han Jie et al ⁹⁶
91.	Demethynobiletin	39.594	0.14	388.4	C ₂₀ H ₂₀ O ₈	358832		anti-inflammatory activity	Guo et al ⁹⁷

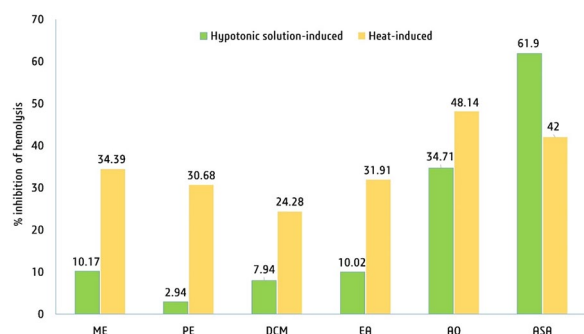


Figure 3. Percentage inhibition of hemolysis of different extracts of peel of *C. reticulata* in hypotonic solution-induced and heat-induced conditions [Here, ME, PE, DCM, EA, and AQ mean the soluble fractions of *C. reticulata* in methanol, pet ether, dichloromethane, ethyl acetate, aqueous conditions, respectively]. Abbreviations: ASA, acetyl salicylic acid.

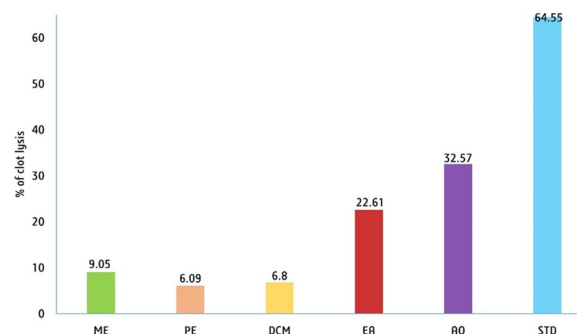


Figure 4. Effects of methanolic crude extract and its various solvent fractions of *C. reticulata* peel against thrombosis [Here, ME, PE, DCM, EA, and AQ mean the soluble fractions of *C. reticulata* in methanol, pet ether, dichloromethane, ethyl acetate, aqueous conditions, respectively]. Abbreviations: ASA, acetyl salicylic acid.

(Stigmasterol), flavonoids (Demethylnobiletin, sinensetin, Pebrellin, and artemetin), and aliphatic cyclic (1,2-Cyclohexanedione, Trimethylene borate, delta-Elementene, and Furaneol) compounds were also identified in this analysis (Table 2).

Antimicrobial properties

Among the fractions DCMSF showed broad spectrum antimicrobial properties. From gram positive bacteria, DCMSF showed 8 mm zone of inhibition at 3 different bacteria such as *B. cereus*, *B. subtilis*, and *S. aureus* while the DCMSF exerted 10 mm zone of inhibition against 3 different gram-negative bacteria such as *S. typhi*, *E. coli*, and *V. parahaemolyticus* at the antimicrobial testing assay (Table S4). DCMSF also showed potency at antifungal *Sarcina lutea* activity, and most effective result was found against *C. albicans* (20 mm zone of inhibition). However, MECE exhibits the poorest zone of inhibition only active against *Sarcina lutea* gram negative bacteria (15 mm; Table S4).

Anti-inflammatory properties

Hypotonic solution-induced hemolysis. In comparison with the standard acetyl salicylic acid at a strength of 0.10 mg/mL (61.90% inhibition against erythrocyte membrane lysis), methanolic extracts of *C. reticulata* peel at a concentration of 2.0 mg/mL revealed a mild protective effect (Figure 3). AQSF, in particular, displayed 34.71% effective inhibition than the other extract.

Heat-induced hemolysis. The extracts from the peel of *C. reticulata* were efficient in erythrocyte lysis triggered by heat according to the outcomes. The inhibition of AQSF was around 48.14%, which is greater than that of MECE (34.39%), EASF (31.91%), PESF (30.68%), and DCMSF (24.28%), and even higher than the standard Acetyl Salicylic Acid (42.0%) under normal conditions (Figure 3).

Thrombolytic properties

Streptokinase (SK), a positive control resulting in a notable 64.55% clot lysis. In contrast, the negative control, treated with distilled water, exhibited minimal clot lysis at 5.64%. However, the AQSF of the peel of *C. reticulata* demonstrated the highest thrombolytic activity at 32.57%, followed by the EASF at 22.61%, DCMSF at 6.80%, MECE at 6.05%, and PESF at 4.06% (Figure 4).

Central analgesic properties

Figure 5a shows the findings of the central analgesic effects of the MECE using the tail immersion technique. The pain reaction time for every sample showed dose-dependent when compared to the control medication, morphine. The 100 and 200 mg/kg body weight doses demonstrated statistically significant central analgesic effects ($P < .05$) at the 30-, 60-, and 90-minute observation points. In contrast, the 400 mg/kg dose showed statistically significant central analgesic effects ($P < .05$) only at the 30-minute observation point (Figure 5a).

Peripheral analgesic properties

The findings of the peripheral analgesic effect of methanolic crude extracts (100, 200, and 400 mg/kg body weight) in mice are shown in Figure 5b. The MECE demonstrated significant efficacy in inhibiting acetic acid-induced abdominal writhing in mice by reducing the number of writhing of mice. After 30 minutes of pain induction, the 100 mg/kg extract reduced pain by 32.18%, while the 400 mg/kg dosage inhibited writhing by 44.83% in mice, compared to the standard diclofenac sodium (77.0% inhibition; Figure S3).

Anti-diarrheal properties

Castor oil-induced diarrhea lasted up to 4 hours in the control group. The anti-diarrheal evaluation of MECE indicated a

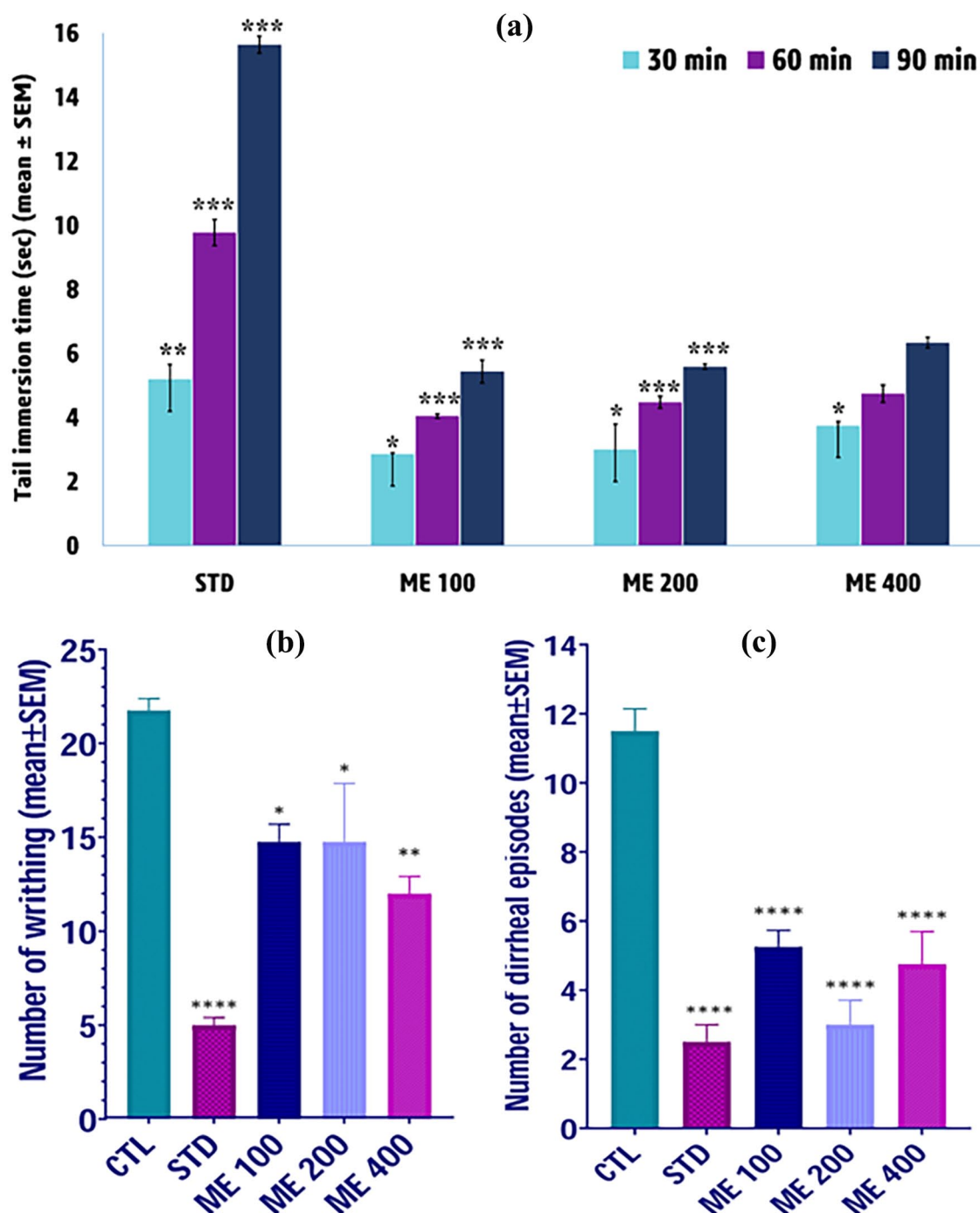


Figure 5. *In vivo* pharmacological actions of MECR: (a) effects of methanolic crude extracts of *C. reticulata* peel on the tail immersion time (seconds) of the mice in central analgesic test, (b) effects of the 3 doses of methanolic crude extract of *C. reticulata* peel on the number of writhing of mice in the peripheral analgesic experiment, (c) effects of the 3 doses of methanolic crude extract of *C. reticulata* peel on the number of diarrheal episodes of mice after 4 hours of administration of Castor oil in antidiarrheal experiment. The data were expressed as mean ± SEM.

*, **, and **** denote $P < .05$, $P < .01$, $P < .001$, and $P < .0001$, respectively versus control group.

very strongly significant ($P < .0001$) antidiarrheal action at various dosages (100, 200, and 400 mg/kg; Figure 5c). Among the studied groups, ME 200 and ME 400 groups showed nearly 70% inhibition in diarrheal episodes at 4 hours (Figure S4), whereas the positive control had a 73.91% reduction in diarrheal episodes at 4 hours (Figure S4).

Molecular docking analysis

Molecular docking studies were performed using various computer-based methods to evaluate the bioactivities of compounds generated from *Citrus reticulata* peel extracts and their solvent fractions. Docking scores, as generated by PyRx, are presented in Figure 6. Supplemental Tables S6–S10 provides

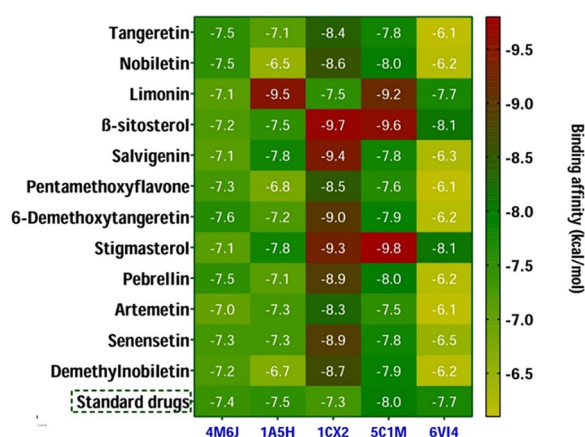


Figure 6. Heat map revealing the binding affinity (kcal/mol) obtained from in silico molecular docking between the isolated compounds and the target receptors. Here, the ciprofloxacin, warfarin, diclofenac, morphine, and loperamide were used as standard drugs while interactions with 4M6J, 1A5H, 1CX2, 4C1M, and 6VI4, respectively.

detailed information on the amino acids interacting with ligand atoms, including the interaction type, distance, and nature. A lower binding affinity value (kcal/mol) indicates stronger binding strength. Optimal docking predictions were identified based on projected binding affinities with a root mean square deviation (RMSD) value of zero. The following sections describe the inhibitory potential of the isolated compounds against specific enzymes and receptors.

Inhibition of dihydrofolate reductase (DHFR). Regarding dihydrofolate reductase (DHFR; 4M6J), all compounds exhibited similar or better binding affinities (-7.0 to -7.6 kcal/mol) when compared to the standard ciprofloxacin (-7.4 kcal/mol). Among them, C-84 had the highest binding affinity (-7.6 kcal/mol), followed by C-A, C-B, and C-87 (each at -7.5 kcal/mol) toward the DHFR protein (Figure 6). The three-dimensional (3D) and two-dimensional (2D) interactions of the best-hit 4 compounds [tangeretin (Compound A), nobiletin (Compound B), 6-Demethoxytangeretin (Compound 84), and pebrellin (Compound 87)] while interacting with DHFR were shown in the Supplemental Figure S5. Predicted interactions were predominantly conventional hydrogen bonds, with some hydrophobic interactions such as pi-alkyl and alkyl bonds also observed (Supplemental Table S6).

Inhibition of tissue plasminogen activator (t-PA). In the case of molecular docking of tissue plasminogen activator (1A5H), compounds C-B, C-83, and C-91 showed lower binding affinities (-6.5 , -6.8 , and -6.7 kcal/mol, respectively) compared to the standard warfarin (-7.5 kcal/mol; Figure 6). However, C-C exhibited the highest binding affinity (-9.5 kcal/mol) among all docked compounds, surpassing warfarin, while the other molecules demonstrated binding affinities close to warfarin (-7.1 to -7.8 kcal/mol; Figure 6). The Supplemental Figure S6 shows the three-dimensional (3D) and two-dimensional (2D) interactions of the best-hit

4 compounds [limonin (Compound C), β -sitosterol (Compound D), salvigenin (Compound 79), and stigmasterol (Compound 86)] while interacting with t-PA revealing anti-thrombotic properties. The interactions noted included hydrophilic (conventional hydrogen bonds and carbon hydrogen bonds) and hydrophobic interactions (alkyl and pi-alkyl; Table S7).

Inhibition of COX-2 enzyme. For cyclooxygenase 2 (1CX2), all docked molecules showed better binding affinities (-9.7 to -7.5 kcal/mol) compared to the positive control diclofenac (-7.3 kcal/mol; Figure 6). Figure 7 exhibited the three-dimensional (3D) and two-dimensional (2D) interactions of the 4 best-hit compounds [β -sitosterol (Compound D), salvigenin (Compound 79), 6-Demethoxytangeretin (Compound 84), and stigmasterol (Compound 86)] while interacting with cyclooxygenase 2 (COX 2) revealing peripheral analgesic properties. The interactions were mostly hydrophobic, involving alkyl and pi-alkyl bonds (Table S8).

Inhibition of mu-opioid receptor. When investigating central analgesic properties via molecular docking analysis with the mu-opioid receptor (5C1M), compounds C, D, and 86 demonstrated more efficient binding affinities (<-9.2 kcal/mol) compared to the standard morphine (-8.0 kcal/mol). The other molecules displayed similar efficiencies (-7.6 to -8.0 kcal/mol) to the positive control (Figure 6). Figure 8 showed the three-dimensional (3D) and two-dimensional (2D) interactions of the 4 best-hit compounds [nobiletin (Compound B), limonin (Compound C), β -sitosterol (Compound D), and stigmasterol (Compound 86)] while interacting with mu-opioid receptor revealing central analgesic properties. Most ligand-protein interactions were hydrophobic, including pi-alkyl and alkyl bonds, with some hydrogen bonds and 1 electrostatic bond also observed (Table S9).

Inhibition of kappa opioid receptor. The compounds β -sitosterol (C-D) and stigmasterol (C-86) exerted the highest binding affinities (-8.1 kcal/mol) toward the kappa opioid receptor than the standard molecule loperamide (-7.7 kcal/mol) revealing their promising antidiarrheal activities (Figure 6). The Supplemental Figure S7 exhibited the three-dimensional (3D) and two-dimensional (2D) interactions of the 4 best-hit compounds [nobiletin (Compound B), limonin (Compound C), β -sitosterol (Compound D), and stigmasterol (Compound 86)] while interacting with kappa opioid receptor revealing antidiarrheal properties. The interactions were predominantly hydrophobic, such as pi-alkyl and alkyl bonds (Supplemental Table S10).

ADMET, physicochemical, and drug-likeness analysis

Poor ADMET profiles are well-known barrier to design effective therapeutic molecule. One of the major challenges in drug development during clinical investigation is addressing these pharmacokinetic characteristics. To overcome these challenges, in silico techniques have been employed to evaluate ADMET properties

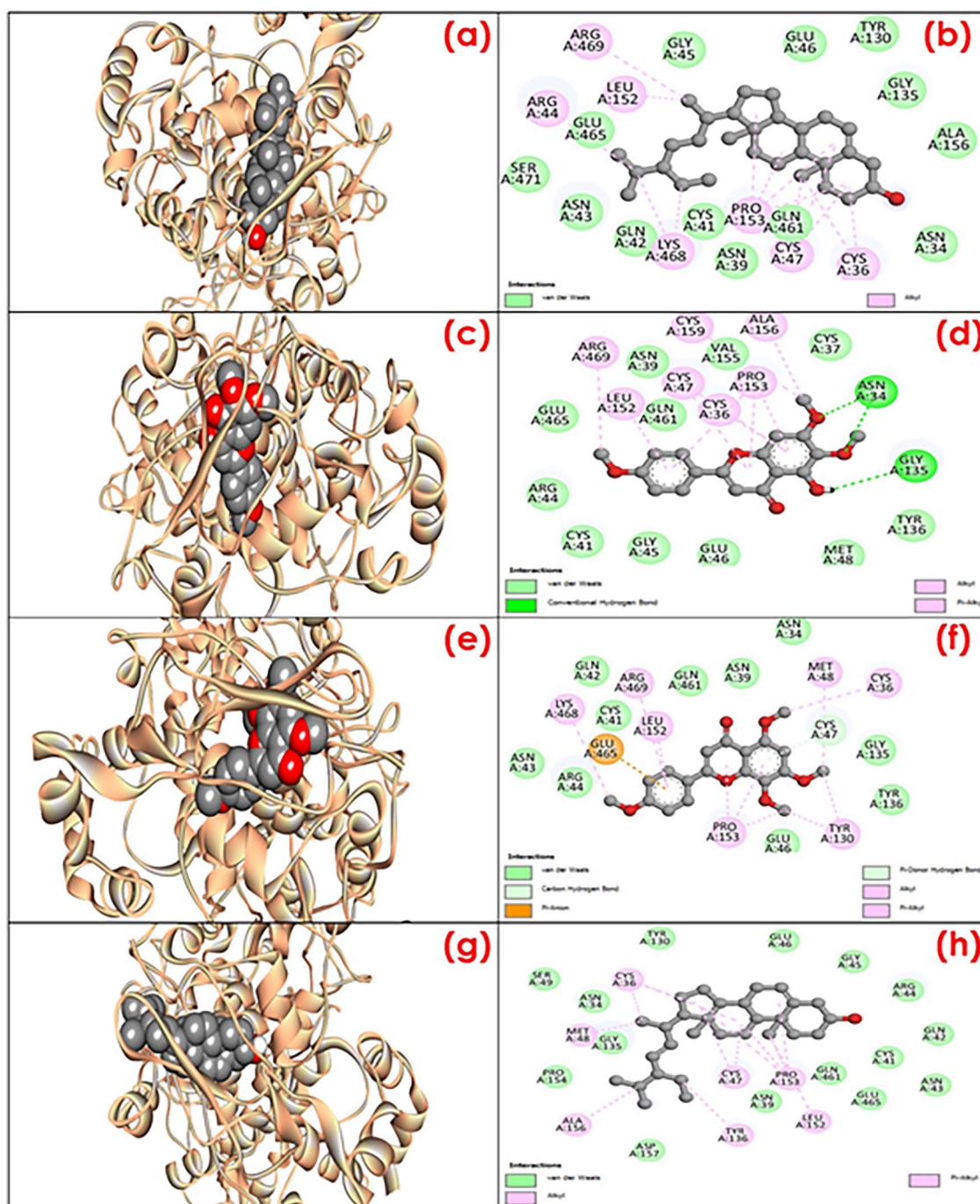


Figure 7. Three-dimensional (3D) and two-dimensional (2D) interactions of the 4 best-hit compounds while interacting with cyclooxygenase 2 (COX-2) revealing peripheral analgesic properties. [Here, (a-h) represent the interactions of β-sitosterol (Compound D), salvigenin (Compound 79), 6-Demethoxytangeretin (Compound 84), and stigmasterol (Compound 86), respectively, while inhibiting the COX-2 protein.].

and predict the drug-likeness of isolated and identified 12 compounds (4 isolated compounds and 8 selected phytochemicals which were detected by GC-MS/MS technique) as potential therapeutic candidates.⁹⁸⁻¹⁰⁰ The results of these ADMET and drug-likeness analyses are summarized in Tables 3 and 4.

Most of the molecules exhibited similar water solubility (3.89 log mol/L), with the exceptions of C-D, C-86, and C-87, which had solubility values of 6.77, 6.68, and 3.47 log mol/L, respectively (Table 3). Nearly all compounds demonstrated

Caco-2 permeability, except for C-87. The phytochemicals also showed comparable human intestinal absorption and skin permeability properties. While C-79, C-87, C-88, and C-91 were not substrates for P-glycoprotein, approximately all other compounds, except for C-87, were able to inhibit P-glycoprotein-I (Table 3). In terms of distribution, most compounds were unbound in a small fraction, except for C-D and C-86, which were fully bound (Table 3). Compounds C-B and C-87 exhibited higher blood-brain barrier (BBB)

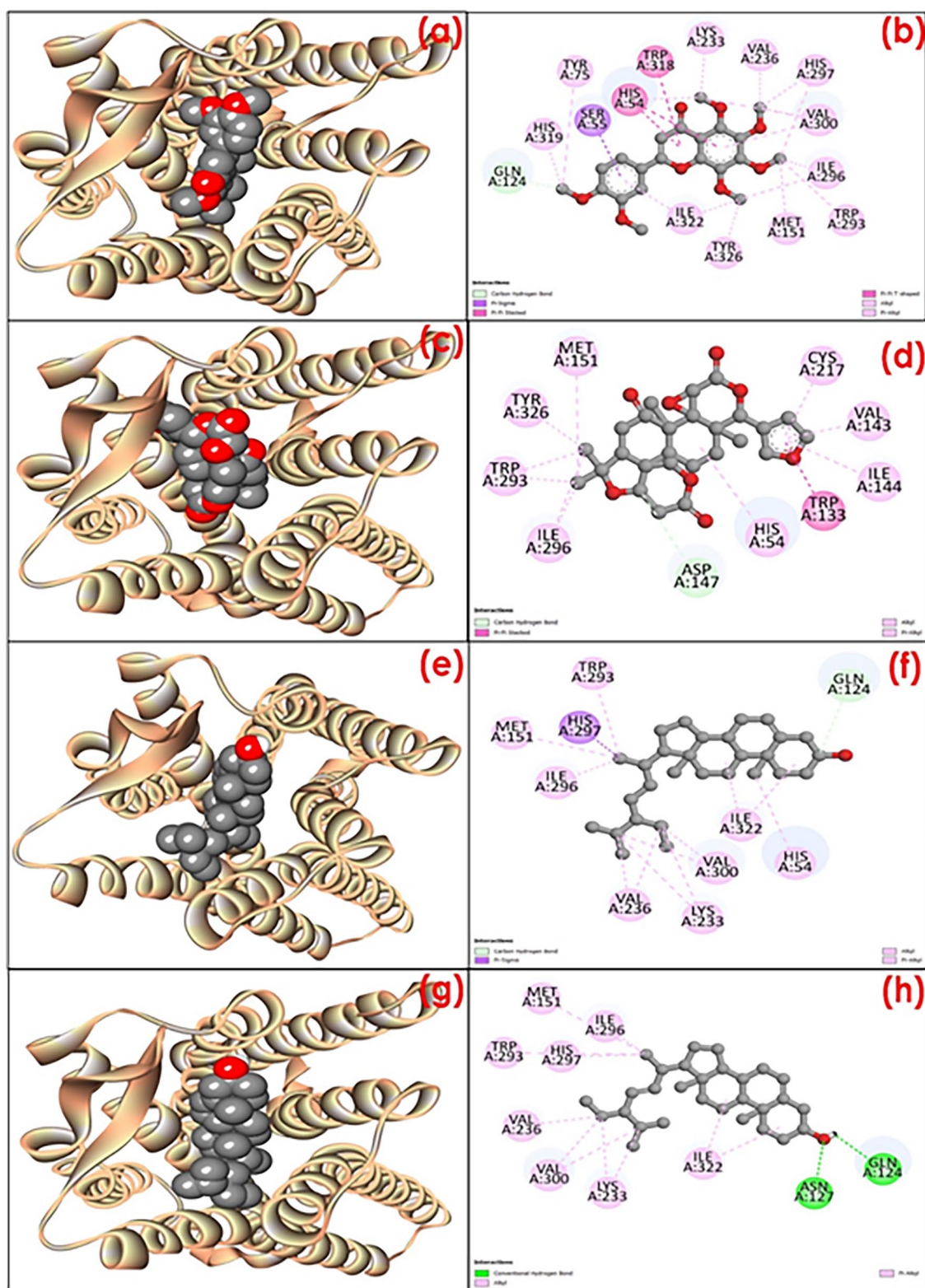


Figure 8. Three-dimensional (3D) and two-dimensional (2D) interactions of the 4 best-hit compounds while interacting with mu-opioid receptor revealing central analgesic properties. [Here, (a-h) represent the interactions of nobiletin (Compound B), limonin (Compound C), β -sitosterol (Compound D), and stigmasterol (Compound 86), respectively, while inhibiting the mu-opioid receptor.].

permeability compared to other molecules. Additionally, all compounds, except for C-D and C-87 (-1.705 and -1.65 , respectively), showed strong central nervous system (CNS) permeability (Table 3). Regarding drug metabolism, all compounds

could act as substrates for CYP2D6 and CYP3A4, except for 87 (Table 3). Compounds C, D, and 86 did not show inhibitory action against any types of CYP450 in the docking study, and no compounds were able to inhibit CYP2D6 (Table 3). For

Table 3. Summary of the parameters regarding the pharmacokinetic and toxicological properties of the lead identified compounds from the peel of *C. reticulata*.

PROPERTIES	MODEL NAME (UNIT)	C-A	C-B	C-C	C-D	C-79	C-83	C-84	C-86	C-87	C-88	C-90	C-91
Absorption	Water solubility (log mol/L)	-4.792	-4.949	-4.04	-6.773	-3.897	-4.794	-4.58	-6.68	-3.479	-4.33	-4.682	-4.32
	Caco2 permeability (log Papp in 10 ⁻⁶ cm/s)	1.245	1.306	0.922	1.201	1.087	1.221	1.171	1.213	0.567	1.424	1.233	1.455
	Intestinal absorption (human; % Absorbed)	98.48	98.92	100	94.46	95.87	98.55	98.25	94.97	97.22	100	98.58	100
	Skin Permeability (log Kp)	-2.678	-2.715	-2.83	-2.78	-2.71	-2.68	-2.62	-2.78	-2.75	-2.75	-2.67	-2.75
	P-glycoprotein substrate	No	No	No	No	Yes	No	No	No	Yes	Yes	No	Yes
Distribution	P-glycoprotein I inhibitor	Yes	Yes	Yes	Yes	Yes	Yes	Yes	Yes	No	Yes	Yes	Yes
	P-glycoprotein II inhibitor	Yes	Yes	No	Yes	Yes	Yes	Yes	Yes	Yes	Yes	Yes	Yes
	VDss (human; log L/kg)	-0.22	-0.28	0.26	0.19	-0.16	-0.22	-0.17	0.17	-0.02	-0.24	-0.18	-0.25
Metabolism	Fraction unbound (human; Fu)	0.188	0.179	0.145	0	0.14	0.195	0.197	0	0.069	0.123	0.155	0.118
	BBB permeability	-1.026	-1.254	-0.84	0.781	-0.695	-1.02	-0.23	0.771	-1.021	-1.15	-1.008	-1.14
	CNS permeability	-3.011	-3.142	-3.07	-1.705	-2.309	-3.032	-2.27	-1.65	-3.198	-3.16	-3.016	-3.17
	CYP2D6 substrate	No	No	No	No	No	No	No	No	No	No	No	No
Excretion	CYP3A4 substrate	Yes	Yes	Yes	Yes	Yes	Yes	Yes	Yes	No	Yes	Yes	Yes
	CYP1A2 inhibitor	Yes	Yes	No	No	Yes	Yes	Yes	No	Yes	Yes	Yes	Yes
	CYP2C19 inhibitor	Yes	Yes	No	No	Yes	Yes	Yes	No	Yes	Yes	Yes	Yes
	CYP2C9 inhibitor	Yes	Yes	No	No	No	Yes	Yes	No	No	Yes	Yes	Yes
	CYP2D6 inhibitor	No	No	No	No	No	No	No	No	No	No	No	No
	CYP3A4 inhibitor	Yes	Yes	No	No	Yes	Yes	No	No	Yes	No	No	Yes
	Total Clearance (log ml/min/kg)	0.78	0.789	0.088	0.628	0.703	0.422	0.791	0.618	0.625	0.706	0.794	0.703
Toxicity	Renal OCT2 substrate	No	No	No	No	Yes	No	No	No	No	No	No	No
	AMES toxicity	No	No	No	No	No	No	No	No	No	No	No	No
	Max. tolerated dose (human; log mg/kg/day)	0.385	0.443	-0.51	-0.621	0.202	0.4	0.295	-0.66	0.293	0.335	0.208	0.336
	hERG I inhibitor	No	No	No	No	No	No	No	No	No	No	No	No
	hERG II inhibitor	No	No	No	Yes	No	No	No	Yes	No	No	No	No
	Oral rat acute toxicity (LD50; mol/kg)	2.368	2.459	3.452	2.552	2.229	2.401	2.29	2.54	2.273	2.36	2.503	2.406
	Oral rat chronic toxicity (LOAEL; log mg/kg_bw/day)	0.944	0.82	1.911	0.855	1.307	0.95	1.095	0.872	1.987	1.025	1.131	1.028
	Hepatotoxicity	No	No	No	No	No	No	No	No	No	No	No	No
	Skin sensitization	No	No	No	No	No	No	No	No	No	No	No	No
	T. Pyriformis toxicity (log µg/L)	0.355	0.315	0.286	0.43	0.481	0.351	0.418	0.433	0.31	0.332	0.384	0.322
Minnow toxicity (log mM)		0.144	0.686	0.446	-1.802	0.856	0.326	-0.2	-1.68	2.331	1.842	0.908	1.842

Table 4. Summary of the parameters regarding the physicochemical properties and drug-likeness qualities.

COMP. NO.	COMPOUND NAME	MOL WEIGHT (G/MOL)	NO. OF ROTATABLE BONDS	H-BOND ACCEPTOR	H-BOND DONOR	MOLAR REFRACTIVITY	TPSA (Å²)	CONSENSUS LOGPO/W	LIPINSKI RULE		BIOAVAILABILITY SCORE
									RESULT	VIOLATION	
C-A	Tangeretin	372.37	6	7	0	100.38	76.36	3.02	Yes	0	0.55
C-B	Nobiletin	402.39	7	8	0	106.87	85.59	3.02	Yes	0	0.55
C-C	Limonin	470.51	1	8	0	116.17	104.57	2.55	Yes	0	0.55
C-D	β-Sitosterol	414.71	1	1	0	133.23	20.23	7.19	Yes	1	0.55
C-79	Salvigenin	328.32	4	6	1	89.42	78.13	2.88	Yes	0	0.55
C-83	Pentamethoxyflavone	372.37	6	7	0	100.38	76.36	3.01	Yes	0	0.55
C-84	6-Demethoxytangeretin	342.34	5	6	0	93.89	67.13	3.00	Yes	0	0.55
C-86	Stigmasterol	412.69	5	1	1	132.75	20.23	6.97	Yes	1	0.55
C-87	Pebrellin	374.34	5	8	2	97.93	107.59	2.43	Yes	0	0.55
C-88	Artemetin	388.37	6	8	1	102.40	96.59	2.82	Yes	0	0.55
C-90	Senensetin	372.37	6	7	0	100.38	76.36	3.10	Yes	0	0.55
C-91	Demethylnobiletin	388.37	6	8	1	102.40	96.59	2.78	Yes	0	0.55

Abbreviations: TPSA, topological polar surface area.

renal clearance, most compounds exhibited total clearance (expressed as log mL/kg/min) ranging from 0.422 to 0.789, except for C-C (0.088). All the compounds acted as non-substrates for renal OCT2 (organic cation transporter 2), excluding C-79 (Table 3). The compounds displayed no AMES toxicity, hERG I inhibition, hERG II inhibition, hepatotoxicity, or skin sensitization (Table 3). According to the OECD 423 model,¹⁰¹ the obtained LD₅₀ values indicated no acute oral toxicity, classifying the substances as class VI ("non-toxic") under the Oral Toxicity Classification. Furthermore, nearly all compounds adhered to Lipinski's rule of 5, with a bioavailability score of 0.55 in the drug-likeness analysis. However, compounds D and 86 had an octanol-water partition coefficient log *P* higher than Lipinski's recommendation (log *P* ≥ 5; Table 4).

Discussion

Fruit plants and vegetables are considered a significant reservoir of bioactive phytochemicals, illustrating various pharmacological properties. Substantial quantities of secondary metabolites are inherent within fruit and vegetable waste or byproducts, thereby the presence of phenolic molecules, dietary fibers, and other biologically active constituents through extraction and isolation techniques can be identified. Scientific research has elucidated the prevalence of phytochemicals and essential nutrients within various components of fruits and vegetables, including peels, seeds, and pulp.¹⁰² The systematic isolation and characterization of these phytochemicals represent a well-recognized approach for identifying bioactive agents derived from fruit waste. Within the phytochemical analysis, several chromatographic methodologies, encompassing column chromatography (CC), thin-layer chromatography (TLC), gas chromatography (GC), and preparative thin-layer chromatography (PTLC), are employed in the purification and refinement of bioactive compounds from botanical extracts. In our study, we conducted a chemical profiling of *Citrus reticulata* fruit peel utilizing methanol as the solvent, employing gel permeation chromatography, TLC screening, and subsequent PTLC analysis. In our study, NMR approaches was applied to confirm the subsequent isolated phytochemical structures in the investigation. Furthermore, GC-MS technique was employed to comprehensively identify additional phytomolecules from the methanolic extract of *C. reticulata* peel.

The present research demonstrated the isolation of 4 compounds from *C. reticulata*, including tangeretin (compound A), nobiletin (compound B), limonin (compound C), and β -sitosterol (compound D), as depicted in Figure 1. These phytochemicals were also detected from the same species reported in previous studies.¹⁰³⁻¹⁰⁵ Nobiletin and tangeretin were separated from the peel extract of *C. reticulata* and reported by Kaushal et al¹⁰⁶ and Mizuno et al,¹⁰⁷ respectively. Additionally, tangeretin and limonin were extracted from the same botanical component and documented by Yaqoob et al.¹⁰⁸ Nevertheless, while β -sitosterol was previously identified and documented in the stem bark

extract,¹⁰⁵ as per our searching experience, this current study represents the first report of its isolation from the *C. reticulata* peel extract. Furthermore, GC-MS approaches detected and characterized over 90 bioactive compounds, notably, D-limonene (antioxidant, antidiabetic, anticancer), emylcamate (anti-cancer, antioxidant), furaneol (antimicrobial), thymine (antibiotics), ethanamine, N-ethyl-nitroso (anticancer), ribitol (anti-microbial), thymol (anti-inflammatory, antiseptic), phytol (cytotoxicity, antioxidant, antimicrobial), β -elemene (antibacterial), humulene (antifungal, anticancer), trehalose (anti-inflammatory), bis (2-ethylhexyl) phthalate (antimicrobial, cytotoxicity), fenoterol (antimicrobial), salvigenin (anti-inflammatory). In addition, many fatty derivatives such as cis,cis,cis - 7,10,13-hexadecatrienal, cis-11-eicosenamide, 9,12-octadecadienoic acid (Z,Z)-, 2,3- dihydroxypropyl ester, and hexadecanoic acid 2-hydroxy1- (hydroxymethyl) ethyl ester were also identified in our phytochemical analysis, which are mainly promising for their antioxidant properties (Table 2).

The assessment of the antibacterial efficacy of the methanolic extract of *C. reticulata* and its assorted fractions was conducted with the aim of identifying novel candidates for antimicrobial agents. This initiative fueled from the escalating issue of resistance exhibited by numerous strains of bacteria against conventional antibiotics, thereby emphasizing the imperative for alternative therapeutics. Additionally, contemporary antibiotic treatments often entail heightened adverse effects, underscoring the urgency to explore alternative avenues for combating bacterial infections.¹⁰⁹ Microorganisms resistant to antimicrobial agents have been identified as the primary causative agents in an estimated 700 000 fatalities annually worldwide. This alarming figure underscores the urgent need for concerted efforts, including discovering novel antibiotics to address antimicrobial resistance.¹¹⁰

The present investigation revealed antibacterial efficacy across various extractives of *C. reticulata*, with notable antimicrobial activity observed specifically within the dichloromethane-soluble fraction. These findings underscore the potential of natural sources such as *C. reticulata* in pursuing novel antimicrobial agents amid the escalating global challenge of antimicrobial resistance.¹¹¹ In addition, the isolated compounds such as tangeretin and nobiletin showed potential antimicrobial activity at several previous studies.¹¹² Moreover, a previous study of the fruit peel showed that the presence of tangeretin and nobiletin exhibited potent antimicrobial activity.¹¹³ Additionally, the isolated compounds demonstrated notable binding affinities toward the dihydrofolate reductase (DHFR) enzyme, with values ranging from -7.0 to -7.6 kcal/mol. These affinities compare favorably to the standard drug ciprofloxacin (-7.4 kcal/mol). In addition, several compounds such as santolina epoxide, 3-(2-piperidinyl) sulfate, β -elemene, α -farnesene, dodecanoic acid, megastigmatrienone, 2,3-anhydro-d-mannosan and isovaleric acid, eicosyl ester were identified through the GC-MS analysis which have anti-microbial properties

(Table 2). Further investigation is needed to establish the exact mechanism of actions of these phytochemicals from the *C. reticulata* fruits peel toward microbial infections.

Thrombosis stands as a leading contributor to morbidity and mortality across a diverse range of vascular dysfunctions.¹¹⁴ By the influence of activated thrombin, fibrinogen undergoes conversion to fibrin, leading to the formation of a thrombus or blood clot. Individuals with occluded veins or arteries receive treatment with fibrinolytic medications, eliminating thrombi by activating tissue plasminogen activator (t-PA) and manifesting a thrombolytic effect.¹¹⁵ Diminishing platelet aggregation serves as a protective measure against specific conditions, such as atherosclerosis.¹¹⁶ In this present investigation, the EASF and AQSF of *C. reticulata* displayed moderate thrombolytic activity (22.61% and 32.57% clot lysis, respectively). Furthermore, a prior study suggests that the identified compound nobiletin could be a promising therapeutic agent for preventing or treating thromboembolic illnesses.¹¹⁷ Another compound, tangeretin, blocks agonist-induced human platelet activation in a concentration-dependent manner. It hinders agonist-induced integrin α IIb β 3 inside-out and outside-in signaling, intracellular calcium mobilization, and granule secretion.¹¹⁸ Furthermore, nearly all the selected compounds from *C. reticulata* for molecular docking exhibited binding affinities toward human tissue plasminogen activator that surpassed those of the standard thrombolytic drug warfarin (−7.5 kcal/mol). The findings from this investigation may contribute to the find out the thrombolytic properties of the fruit peel of *C. reticulata*.^{119,120}

Substances capable of stabilizing the erythrocyte membrane may also stabilize the lysosomal membrane, thereby exhibiting anti-inflammatory properties by influencing the activity and release of cell mediators due to their structural similarities.^{25,121} In this context, the AQSF of *C. reticulata* showcased notable anti-inflammatory efficacy by averting erythrocyte hemolysis in conditions induced by both hypotonic solution and heat. GC-MS analysis revealed the presence of several anti-inflammatory compounds in MECR, including α -farnesene, dl-citrulline, trehalose, ethyl cholate, octadecanamide, salvigenin, vitamin E, sinensetin, and demethylnobiletin. Furthermore, a compound like limonin exhibited potent inhibition of IL-1 β -Induced Inflammation, mitigating osteoarthritis inflammation by activating Nrf2.¹²² Additionally, all the docking compounds demonstrated the enhanced binding affinities for the cyclooxygenase protein (COX 2), which supports the outcomes of the experimental studies. Plausibly, these molecules might be accountable for the anti-inflammatory activity of *C. reticulata*. Additional investigations should be conducted to isolate and identify the specific molecules responsible for the membrane-stabilizing properties.

Exploration for pain-alleviating substances is emphasized from natural reservoirs as substitutes for synthetic medications due to their lower adverse effects.¹²³ The current investigation revealed the analgesic potential of the methanol

extract from the peel of *C. reticulata* using the writhing and tail immersion methods in mice. In our experimental setting, the plant extract mitigated acetic acid-induced pain responses in mice more effectively than heat-induced pain reactions. The findings propose that phytochemicals within the fruit peel extracts of *C. reticulata* may possess the capability to diminish pain by impeding prostaglandin synthesis.^{124,125} Some of the isolated and detected compounds of this phytochemical investigation showed high binding affinity than the conventional analgesic medicine morphine and diclofenac. One prior study indicated that the isolated compound β -sitosterol exhibited analgesic effects in hot plate and acetic acid-induced assessments by either inhibiting central opioid receptors or facilitating the release of endogenous opioid peptides, and inhibiting the production of prostaglandins and bradykinins.¹²⁶ Furthermore, the GC-MS technique detected certain analgesic compounds such as gamma-Terpinene, Linalool, and Benzofuran, 2,3-dihydro, suggesting the fruit peel of *C. reticulata* possesses analgesic attributes.

Since time immemorial, medicinal flora has been utilized to address various gastrointestinal (GI) disorders, such as diarrhea. Nonetheless, the safety and effectiveness profiles of the majority of these botanicals have not been scrutinized. As a result, this investigation was done to assess the efficacy of the peel extract of *C. reticulata* fruits as a potential remedy for diarrhea. Ricinoleic acid, the primary element in castor oil, is known to provoke irritation of the intestinal wall, eliciting peristaltic motion and ultimately leading to diarrhea.¹²⁷ The MECR of *C. reticulata* exhibited significant properties to counteract diarrhea. Even the smaller dosage (100 mg/kg bw) displayed a significant antidiarrheal effect. This exploration illustrated that the anti-diarrheal capabilities of the MECR could be ascribed to the bioactive phytochemicals accountable for the anti-diarrheal effect.¹²⁸ Molecular docking displayed that 3 compounds C, D, and 86 had higher binding affinities than the standard drug loperamide. β -Sitosterol, an isolated secondary metabolite from *C. reticulata*, might assume a significant function in diminishing peristalsis in the GI system, consequently averting GI motility.^{127,128} While the GC-MS method did not reveal any potent antidiarrheal phytomolecules, according to the literature pharmacological activities records, antioxidant compounds may be instrumental in mitigating intestinal motility.¹²⁹ These antioxidant agents could alleviate the impact of castor oil-induced intestinal inflammation while several antioxidant compounds were identified through the GC-MS approach. Furthermore, 2 flavonoid molecules, tangeretin, and nobiletin, possess potent antioxidant attributes.^{130,131}

Limitations and future research

The current study presents certain limitations and gaps. The purified compounds were not pharmacologically investigated.

Instead, the study reported their actions computationally to support the pharmacological properties of the MECR and its various solvent fractions. Nevertheless, the study will serve as a foundation for future research focused on the extensive phytochemical isolation of additional polymethoxyflavones and other flavonoids and their pharmacological evaluations. Moreover, it is recommended that the most abundant purified polymethoxyflavones be assessed for their potential effectiveness against chronic disorders, including infections, thrombosis, inflammation, pain, and diarrhea, based on the present evidence. Additionally, the MECR has not been subjected to acute, subacute, or chronic toxicity evaluations in this report, which should be addressed in future studies.

Conclusion

The present study successfully identified and isolated four purified compounds: tangeretin, nobiletin, limonin, and β -sitosterol, utilizing column chromatography, TLC, and NMR spectroscopic techniques. Additionally, the study detected over 90 phytoconstituents in the fruit peel extract of *Citrus reticulata* through GC-MS/MS analysis. The study also evaluated the pharmacological properties of the peel extract of *C. reticulata*, focusing on antibacterial, thrombolytic, anti-inflammatory, analgesic, and antidiarrheal activities. Promising *in vitro* antimicrobial and anti-inflammatory properties were exhibited by the methanolic fruit peel extract and its various solvent fractions. Statistically significant *in vivo* peripheral analgesic and antidiarrheal effects were observed with the crude extract at the tested doses (100, 200, and 400 mg/kg bw), where the outcomes were further supported by *in silico* investigations. In addition, the reported promising compounds demonstrated favorable pharmacokinetics and safety profiles, which are essential for the development of new drugs. The presence of various polymethoxyflavones in this plant underlines the numerous therapeutic benefits of *C. reticulata* fruit peels. However, additional research is needed to fully understand the precise mechanisms and discover the bioactive compounds that govern the actions of *C. reticulata* through a combined experimental and computational approach.

Acknowledgements

We extend our gratitude to the Department of Pharmacy at the State University of Bangladesh for the laboratory facilities and logistical support essential for conducting this research.

Ethics

The protocols for animal handling and procedures involved in the animal studies were thoroughly reviewed and approved by the Animal Ethics Committee at the State University of Bangladesh, Dhaka, Bangladesh (approval number: 2022-01-23/SUB/A-ERC/006).

Informed Consent

Not required.

ORCID iDs

Md. Jamal Hossain  <https://orcid.org/0000-0001-9706-207X>

Md. Abdus Samadd  <https://orcid.org/0000-0002-8287-5454>

Md. Shohel Hossen  <https://orcid.org/0009-0000-8435-9712>

Data Availability Statement

Data included in article/supp. material/referenced in article.

Supplemental Material

Supplemental material for this article is available online.

REFERENCES

- George P. Concerns regarding the safety and toxicity of medicinal plants-an overview. *J Appl Pharm Sci.* 2011;1:40-44.
- Sahoo N, Manchikanti P. Herbal drug regulation and commercialization: an Indian industry perspective. *J Altern Complement Med.* 2013;19:957-963.
- Yuan H, Ma Q, Ye L, Piao G. The traditional medicine and modern medicine from natural products. *Molecules.* 2016;21:559.
- Anand U, Jacobo-Herrera N, Altemimi A, Lakhssassi N. A comprehensive review on medicinal plants as antimicrobial therapeutics: potential avenues of biocompatible drug discovery. *Metabolites.* 2019;9:258.
- Bayrakçeken Güven Z, Saracoglu I, Nagatsu A, Yilmaz MA, Basaran AA. Anti-tyrosinase and antimelanogenic effect of cinnamic acid derivatives from *Prunus mahaleb* L.: phenolic composition, isolation, identification and inhibitory activity. *J Ethnopharmacol.* 2023;310:116378.
- Pandey MM, Rastogi S, Rawat AK. Indian traditional ayurvedic system of medicine and nutritional supplementation. *Evid Based Complement Alternat Med.* 2013;2013:376327.
- Atanasov AG, Zotchev SB, Dirsch VM, Supuran CT. Natural products in drug discovery: advances and opportunities. *Nat Rev Drug Discov.* 2021;20:200-216.
- Nasim N, Sandeep IS, Mohanty S. Plant-derived natural products for drug discovery: current approaches and prospects. *Nucleus.* 2022;65:399-411.
- Riaz M, Rasool N, Bukhari IH, Shahid M, Zubair K, Rizwan U. In vitro antimicrobial, antioxidant, cytotoxicity and GC-MS analysis of *Mazus goodenifolius*. *Molecules.* 2012;17:14275-14278.
- Mesa C, Ranalison O, Randriantseheno LN, Risuleo G. Natural products from Madagascar, socio-cultural usage, and potential applications in advanced biomedicine: a concise review. *Molecules.* 2021;26:4507.
- Sultana A, Hossain MJ, Kuddus MR, et al. Ethnobotanical uses, phytochemistry, toxicology, and pharmacological properties of *Euphorbia neriifolia* linn. against infectious diseases: a comprehensive review. *Molecules.* 2022;27:4374.
- Sawamura M, Thi Minh Tu N, Onishi Y, Ogawa E, Choi H-S. Characteristic odor components of citrus reticulata Blanco (Ponkan) cold-pressed oil. *Biosci Biotechnol Biochem.* 2004;68:1690-1697.
- Shorbagi M, Fayek NM, Shao P, Farag MA. Citrus reticulata Blanco (the common mandarin) fruit: an updated review of its bioactive, extraction types, food quality, therapeutic merits, and bio-waste valorization practices to maximize its economic value. *Food Biosci.* 2022;47:101699.
- Chopra RN, Nayar SL, Chopra IC. *Glossary of Indian Medicinal Plants (including the Supplement)*. Council of Scientific and Industrial Research. 1986:77-100.
- Khan MA, Ali M, Alam P. Phytochemical investigation of the fruit peels of *Citrus reticulata* Blanco. *Nat Prod Res.* 2010;24:610-620.
- Zou Z, Xi W, Hu Y, Nie C, Zhou Z. Antioxidant activity of citrus fruits. *Food Chem.* 2016;196:885-896.
- Apraj VD, Pandita NS. Evaluation of skin anti-aging potential of citrus reticulata Blanco peel. *Pharmacogn Res.* 2016;8:160-168.
- Sultana HS, Ali M, Panda BP. Influence of volatile constituents of fruit peels of citrus reticulata Blanco on clinically isolated pathogenic microorganisms under in-vitro. *Asian Pac J Trop Biomed.* 2012;2:S1299-1302.

19. Liu Y, Heying E, Tanumihardjo SA. History, global distribution, and nutritional importance of citrus fruits. *Compr Rev Food Sci Food Saf*. 2012;11:530-545.
20. Li S, Pan MH, Lo CY, et al. Chemistry and health effects of polymethoxyflavones and hydroxylated polymethoxyflavones. *J Funct Foods*. 2009;1:2-12.
21. Guo J, Tao H, Cao Y, Ho C-T, Jin S, Huang Q. Prevention of obesity and Type 2 diabetes with aged Citrus Peel (Chenpi) extract. *J Agric Food Chem*. 2016;64:2053-2061.
22. VanWagenen BC, Larsen R, Cardellina JH, Randazzo D, Lidert ZC, Swithenbank C. Ulosantoin, a potent insecticide from the sponge *Ulosa ruetzleri*. *J Org Chem*. 1993;58:335-337.
23. Rashid PT, Hossain MJ, Zahan MS, et al. Chemico-pharmacological and computational studies of *Ophiorrhiza fasciculata* D. Don and *Psychotria silhetensis* hook. f. focusing cytotoxic, thrombolytic, anti-inflammatory, antioxidant, and antibacterial properties. *Heliyon*. 2023;9:e20100.
24. Bauer AW, Kirby WMM, Sherris JC, Turck M. Antibiotic susceptibility testing by a standardized single disk method. *Am J Clin Pathol*. 1966;45:493-496.
25. Debnath PC, Das A, Islam A, Islam MA, Hassan MM, Gias Uddin SM. Membrane stabilization—a possible mechanism of action for the anti-inflammatory activity of a Bangladeshi medicinal plant: *Erioglossum rubiginosum* (Bara Harina). *Pharmacogn J*. 2013;5:104-107.
26. Prasad S, Kashyap RS, Deopujari JY, Purohit HJ, Taori GM, Dagainawala HF. Development of an in vitro model to study clot lysis activity of thrombolytic drugs. *Thromb J*. 2006;4:14.
27. Percie du Sert N, Hurst V, Ahluwalia A, et al. The ARRIVE guidelines 2.0: updated guidelines for reporting animal research. *J Cereb Blood Flow Metab*. 2020;40:1769-1777.
28. Bulbul IJ, Hossain MJ, Haque MR, et al. Two rare flavonoid glycosides from *Litsea glutinosa* (Lour.) CB Rob.: experimental and computational approaches endorse antidiabetic potentiality. *BMC Complement Med Ther*. 2024;24:69.
29. Mukta MM, Hossain MJ, Akter M, et al. Cardioprotection of water spinach (*Ipomoea aquatica*), wood apple (*Limonia acidissima*) and linseed (*Linum usitatissimum* L.) on doxorubicin-induced cardiotoxicity and oxidative stress in rat model. *Nutr Metab Insights*. 2023;16:11786388231212116.
30. Rahman MM, Soma MA, Sultana N, et al. Exploring therapeutic potential of *Woodfordia fruticosa* (L.) Kurz leaf and bark focusing on antioxidant, anti-thrombotic, antimicrobial, anti-inflammatory, analgesic, and antidiarrheal properties. *Health Sci. Rep*. 2023;6:e1654.
31. Ezeja M, Omeh Y, Ezeigbo I, Ekechukwu A. Evaluation of the analgesic activity of the methanolic stem bark extract of *Dialium guineense* (Wild). *Ann Med Health Sci Res*. 2011;1:55-62.
32. Ameer KNS, Hossain MJ, Rohoman A, et al. Phytochemical and pharmacological profiling of extracts of *Pterygota alata* (Roxb.) R. Br. Leaves deciphered therapeutic potentialities against pain, hyperglycemia and diarrhea via in vivo approaches. *Pharmacol Res*. 2024;4:100060.
33. Deng J, Han J, Chen J, et al. Comparison of analgesic activities of aconitine in different mice pain models. *PLoS One*. 2021;16:e0249276.
34. Sisay M, Engidawork E, Shibeshi W. Evaluation of the antidiarrheal activity of the leaf extracts of *Myrtus communis* linn (Myrtaceae) in mice model. *BMC Complement Altern Med*. 2017;17:103.
35. Shoba FG, Thomas M. Study of antidiarrhoeal activity of four medicinal plants in castor-oil induced diarrhoea. *J Ethnopharmacol*. 2001;76:73-76.
36. Dallakyan S, Olson AJ. Small-molecule library screening by docking with pyrx. *Methods Mol Biol*. 2015;1263:243-250.
37. Taher MA, Hossain MJ, Zahan MS, et al. Phyto-pharmacological and computational profiling of *Bombax ceiba* linn. leaves revealed pharmacological properties against oxidation, hyperglycemia, pain, and diarrhea. *Heliyon*. 2024;10:e35422.
38. Lekmine S, Benslama O, Kadi K, et al. LC/MS-MS analysis of phenolic compounds in *Hyoscyamus albus* L. extract: in vitro antidiabetic activity, in silico molecular docking, and in vivo investigation against STZ-induced diabetic mice. *Pharmaceutics*. 2023;16:1015.
39. Talci TE, Fatimawali, Adam AA, et al. Fruit Bromelain-derived peptide potentially restrains the attachment of SARS-CoV-2 variants to hACE2: a pharmacoinformatics approach. *Molecules*. 2022;27:260.
40. Bikadi Z, Hazai E. Application of the PM6 semi-empirical method to modeling proteins enhances docking accuracy of AutoDock. *J Cheminform*. 2009;1:15.
41. Farzana M, Hossain MJ, El-Shehawi AM, et al. Phenolic constituents from *Wendlandia tinctoria* var. *grandis* (Roxb.) DC. stem deciphering pharmacological potentials against oxidation, hyperglycemia, and diarrhea: phyto-pharmacological and computational approaches. *Molecules*. 2022;27:5957.
42. Jannat T, Hossain MJ, El-Shehawi AM, et al. Chemical and pharmacological profiling of *Wrightia coccinea* (roxb. Ex hornem.) Sims focusing antioxidant, cytotoxic, antidiarrheal, hypoglycemic, and analgesic properties. *Molecules*. 2022;27:4024.
43. Khatun MCS, Muhit MA, Hossain MJ, Al-Mansur MA, Rahman SMA. Isolation of phytochemical constituents from *Stevia rebaudiana* (Bert.) and evaluation of their anticancer, antimicrobial and antioxidant properties via in vitro and in silico approaches. *Heliyon*. 2021;7:e08475.
44. Kaplan W, Littlejohn TG. Swiss-PDB viewer (deep view). *Brief Bioinform*. 2001;2:195-197.
45. Assel M, Sjöberg D, Elders A, et al. Guidelines for reporting of statistics for clinical research in urology. *BJU Int*. 2019;123:401-410.
46. Morimoto M, Kumeda S, Komai K. Insect antifeedant flavonoids from *Gnaphalium affine* D. Don. *J Agric Food Chem*. 2000;48:1888-1891.
47. Santos JS, Escher GB, da Silva Pereira JM, et al. ¹H NMR combined with chemometrics tools for rapid characterization of edible oils and their biological properties. *Ind Crops Prod*. 2018;116:191-200.
48. Breksa API, Dragull K, Wong RY. Isolation and identification of the first C-17 limonin epimer, epilimonin. *J Agric Food Chem*. 2008;56:5595-5598.
49. Majid Shah S, Ullah F, Ayaz M, et al. β -sitosterol from *Ilfoja spicata* (Forssk.) sch. bip. as potential anti-leishmanial agent against *leishmania tropica*: docking and molecular insights. *Steroids*. 2019;148:56-62.
50. Chukwu C, Omaka O, Aja P. Characterization of 2,5-dimethyl-2,4-dihydroxy-3(2H) furanone, a flavourant principle from *Sysepalum dulcificum*. *Nat Prod Chem Res*. 2017;5:8. doi:10.4172/2329-6836.1000299
51. Anandakumar P, Kamaraj S, Vanitha MK. D-limonene: a multifunctional compound with potent therapeutic effects. *J Food Biochem*. 2021;45:e13566.
52. Zhang L-L, Chen Y, Li Z-J, Li X, Fan G. Bioactive properties of the aromatic molecules of spearmint (*Mentha spicata* L.) essential oil: a review. *Food Funct*. 2022;13:3110-3132.
53. Onyegeme-Okerenta BM, Minadoki MD, Amadi BA. Phytochemical composition and antiparasmodial potential of fruit extract of *Hunteria umbellata* on chloroquine-sensitive plasmodium berghei berghei (NK65)-infected Albino Mice. *Asian J Emerg. Res*. 2023;5:9-21.
54. Laribi B, Kouki K, M'Hamdi M, Bettaieb T. Coriander (*Coriandrum sativum* L.) and its bioactive constituents. *Fitoterapia*. 2015;103:9-26.
55. Sung WS, Jung HJ, Lee IS, Kim HS, Lee DG. Antimicrobial effect of furaneol against human pathogenic bacteria and fungi. *J Microbiol Biotechnol*. 2006;16:349-354.
56. Liu Y, Yang K, Jia Y, Shi J, Tong Z, Wang Z. Thymine sensitizes Gram-negative pathogens to antibiotic killing. *Front Microbiol*. 2021;12:622798.
57. Fujisawa S, Ishihara M, Murakami Y, Atsumi T, Kadoma Y, Yokoe I. Predicting the biological activities of 2-methoxyphenol antioxidants: effects of dimers. *In Vivo*. 2007;21:181-188.
58. Ambati R, Phang SM, Ravi S, Aswathanarayana R. Astaxanthin: sources, extraction, stability, biological activities and its commercial applications—a review. *Mar Drugs*. 2014;12:128-152.
59. Mehani M, Segni L, Terzi V, et al. Antibacterial, antifungal activity and chemical composition study of essential oil of *Mentha piperita* from the south Algerian. *Der Pharma Chemica*. 2015;7:382-387.
60. Chen Z, Liu Q, Zhao Z, et al. Effect of hydroxyl on antioxidant properties of 2,3-dihydro-3,5-dihydroxy-6-methyl-4 H -pyran-4-one to scavenge free radicals. *RSC Adv*. 2021;11:34456-34461.
61. Zamakshshari NH, Ahmed IA, Didik NAM, Nasharuddin MNA, Hashim NM, Abdullah R. Chemical profile and antimicrobial activity of essential oil and methanol extract from peels of four *Durio zibethinus* L. varieties. *Biomass Convers Biorefinery*. 2023;13:13995-14003.
62. Montague W, Taylor KW. The role of the pentose phosphate pathway in insulin secretion. In: Falkmer S, Hellman B, Täljedal IB, eds. *The Structure and Metabolism of the Pancreatic Islets*. Pergamon Press; 1970:263-273.
63. Mondello F, Fontana S, Scaturro M, et al. Terpinen-4-ol, the main bioactive component of Tea Tree Oil, as an innovative antimicrobial agent against *Legionella pneumophila*. *Pathogens*. 2022;11:682.
64. Khaleel C, Tabanca N, Buchbauer G. α -terpineol, a natural monoterpene: a review of its biological properties. *Open Chem*. 2018;16:349-361.
65. Khodarahmi G, Asadi P, Hassanzadeh F, Khodarahmi E. Benzofuran as a promising scaffold for the synthesis of antimicrobial and antibreast cancer agents: a review. *J Res Med Sci*. 2015;20:1094-1104.
66. Erwin, Pratiwi DR, Saputra I, Alimuddin. Antioxidant assay with scavenging DPPH radical of *Artocarpus anisophyllus* Miq Stem bark extracts and chemical compositions and toxicity evaluation for the most active fraction. *Res J Pharm Technol*. 2021;14:2819-2823.
67. Zhao L, Chen J, Su J, et al. In vitro antioxidant and antiproliferative activities of 5-hydroxymethylfurfural. *J Agric Food Chem*. 2013;61:10604-10611.
68. Bouyahya A, Mechchate H, Benali T, et al. Health benefits and pharmacological properties of carvone. *Biomolecules*. 2021;11:1803.
69. Naksing T, Teeka J, Rattanavichai W, Pongthai P, Kaewpa D, Areesirisuk A. Determination of bioactive compounds, antimicrobial activity, and the phytochemistry of the organic banana peel in Thailand. *J Biosci*. 2021;37:1981-3163.
70. Faizan M, Tonny SH, Afzal S, et al. β -cyclocitral: emerging bioactive compound in plants. *Molecules*. 2022;27:6845.

71. Marchese A, Orhan IE, Daglia M, et al. Antibacterial and antifungal activities of thymol: a brief review of the literature. *Food Chem.* 2016;210:402-414.
72. Jeong JB, Jeong HJ. 2-Methoxy-4-vinylphenol can induce cell cycle arrest by blocking the hyper-phosphorylation of retinoblastoma protein in benzo[a]pyrene-treated NIH3T3 cells. *Biochem Biophys Res Commun.* 2010;400:752-757.
73. Islam MT, Ali ES, Uddin SJ, et al. Phytol: a review of biomedical activities. *Food Chem Toxicol.* 2018;121:82-94.
74. Shamsizadeh A, Roobakhsh A, Ayoobi F, Moghaddamhamdi A. Chapter 25 - the role of natural products in the Prevention and treatment of Multiple Sclerosis. In: Watson RR, Killgore WDS, eds. *Nutrition and Lifestyle in Neurological Autoimmune Diseases*. Academic Press; 2017:249-260.
75. Tamer CE, Suna S, Özcan-Sinir G. 14 - Toxicological aspects of ingredients used in nonalcoholic beverages. In: Grumezescu AM, Holban AM, eds. *Non-alcohol*. Woodhead Publishing; 2019:441-481.
76. Russo EB, Marcu J. Chapter three - cannabis pharmacology: the usual suspects and a few promising leads. *Adv Pharmacol.* 2017;80:67-134.
77. Habibah A, Zahira G, Angga M, Nishfatul S, Rokhim D. Schematic literature review: content of A-farnesene compounds as an anti-virus. *Manganite: J Chem Edu.* 2023;2:24-29.
78. Dubey MK, Aamir M, Kaushik MS, et al. PR toxin - biosynthesis, genetic regulation, toxicological potential, prevention and control measures: overview and challenges. *Front Pharmacol.* 2018;9:288.
79. Mazumder K, Nabila A, Aktar A, Farahnaky A. Bioactive variability and in vitro and in vivo antioxidant activity of unprocessed and processed flour of nine cultivars of Australian lupin species: a comprehensive substantiation. *Antioxidants.* 2020;9:282.
80. Choi J, Shin K-M, Park H-J, et al. Anti-inflammatory and antinociceptive effects of sinapyl alcohol and its glucoside syringin. *Planta Med.* 2004;70:1027-1032.
81. Frapporti G, Colombo E, Ahmed H, et al. Squalene-based nano-assemblies improve the pro-autophagic activity of trehalose. *Pharmaceutics.* 2022;14:862.
82. Al-Otaibi SN, Alshammari GM, AlMohanna FH, Al-Khalifa AS, Yahya MA. Antihyperlipidemic and hepatic antioxidant effects of leek leaf methanol extract in high fat diet-fed rats. *Life.* 2020;13:373-385.
83. Rossellia S, Maggio A, Formisano C, et al. Chemical composition and antibacterial activity of extracts of *Helleborus boccone* ten. subsp. *intermedius*. *Nat Prod Commun.* 2007;2:1934578X0700200611.
84. Ali HAM, Imad HH, Salah AI. Analysis of bioactive chemical components of two medicinal plants (*Coriandrum sativum* and *Melia azedarach*) leaves using gas chromatography-mass spectrometry (GC-MS). *Afr J Biotechnol.* 2015;14:2812-2830.
85. Habib MR, Karim MR. Antimicrobial and cytotoxic activity of Di-(2-ethyl-hexyl) phthalate and anhydrosophoradiol-3-acetate isolated from *Calotropis gigantea* (Linn.) flower. *Mycobiology.* 2009;37:31-36.
86. Kim SK, Karadeniz F. Chapter 14 - biological importance and applications of squalene and squalane. In: Kim SK, ed. *Advances in Food and Nutrition Research*. Academic Press; 2012:223-233.
87. Soliman M, Mohamed G, Mohamed E. Metal complexes of fenoterol drug: preparation, spectroscopic, thermal, and biological activity characterization. *J Therm Anal Calorim.* 2009;99:639-647.
88. Sánchez-Illana JD, Piñeiro-Ramos V, Ramos-García I, Ten-Doménech M, Vento J, Kuligowski. Chapter three - oxidative stress biomarkers in the preterm infant. In: Makowski GS, ed. *Advances in Clinical Chemistry*. Elsevier; 2021:127-189.
89. Mansourabadi AH, Sadeghi H, Razavi N, Rezvani E. Anti-inflammatory and analgesic properties of salvigenin, *Salvia officinalis* flavonoid extracted. *Adv Herb Med.* 2015;1:31-41.
90. Hung W-L, Chang W-S, Lu W-C, et al. Pharmacokinetics, bioavailability, tissue distribution and excretion of tangeretin in rat. *J Food Drug Anal.* 2018;26:849-857.
91. Li S, Wang H, Guo L, Zhao H, Ho C-T. Chemistry and bioactivity of nobiletin and its metabolites. *J Funct Foods.* 2014;6:2-10.
92. García-Moreno M, Moreno-Conesa M, Rodríguez-López JN, García-Cánovas F, Varón R. Oxidation of 4-tert-butylcatechol and dopamine by hydrogen peroxide catalysed by Horseradish peroxidase. *Biol Chem.* 1999;380:689-694.
93. Hossain MJ, Lema KR, Samadd MA, Aktar R, Rashid MA, Al-Mansur MA. Chemical profiling and antioxidant, Anti-Inflammatory, cytotoxic, analgesic, and antiarthralgic activities from the seeds of commonly available red grape (*Vitis vinifera* L.). *Nutr Metab Insights.* 2024;17:11786388241275100.
94. Mamadalieva NZ, Hussain H, Xiao J. Recent advances in genus *Mentha*: phytochemistry, antimicrobial effects, and food applications. *Food Front.* 2020;1:435-458.
95. Bayeux MC, Fernandes AT, Foglio MA, Carvalho JE. Evaluation of the anti-dematogenic activity of artemetin isolated from *Cordia curassavica* DC. *Asian J Med Biol Res.* 2002;35:1229-1232.
96. Han Jie L, Jantan I, Yusoff SD, Jalil J, Husain K. Sinensetin: an insight on its pharmacological activities, mechanisms of action and toxicity. *Front Pharmacol.* 2021;11:553404.
97. Guo S, Wu X, Zheng J, Song M, Dong P, Xiao H. Anti-inflammatory property of 5-Demethylnobiletin (5-hydroxy-6, 7, 8, 3', 4'-pentamethoxyflavone) and its metabolites in lipopolysaccharide (LPS)-Induced RAW 264.7 cells. *Biology.* 2022;11:1820.
98. Kandsi F, Elbouzidi A, Lafdil FZ, et al. Antibacterial and antioxidant activity of *Dysphania ambrosioides* (L.) Mosyakin and clematis essential oils: experimental and computational approaches. *Antibiotics.* 2022;11:482.
99. Kandsi F, Lafdil FZ, Elbouzidi A, et al. Evaluation of acute and subacute toxicity and LC-MS/MS compositional alkaloid determination of the hydroethanolic extract of *Dysphania ambrosioides* (L.) Mosyakin and clematis flowers. *Toxins.* 2022;14:475.
100. Pires DE, Blundell TL, Ascher DB. Ascher, pkCSM: predicting small-molecule pharmacokinetic and toxicity properties using graph-based signatures. *J Med Chem.* 2015;58:4066-4072.
101. OECD. *Test No. 423: Acute Oral toxicity - Acute Toxic Class Method*. Organisation for Economic Co-operation and Development; 2002. Accessed June 5, 2024. https://www.oecd.org/en/publications/test-no-423-acute-oral-toxicity-acute-toxic-class-method_9789264071001-en.html
102. Hussain H, Mamadalieva NZ, Hussain A, et al. Fruit peels: food waste as a valuable source of bioactive natural products for drug discovery. *Curr Issues Mol Biol.* 2022;44:1960-1994.
103. Liu J, Liu C, Rong Y, Huang G, Rong L. Extraction of limonin from Orange (*Citrus reticulata* Blanco) seeds by the Flash extraction method. *Solvent Extr Res Dev Jpn.* 2012;19:137-145.
104. Nakajima A, Nemoto K, Ohizumi Y. An evaluation of the genotoxicity and sub-chronic toxicity of the peel extract of Ponkan cultivar 'Ohta ponkan' (*Citrus reticulata* Blanco) that is rich in nobiletin and tangeretin with anti-dementia activity. *Regul Toxicol Pharmacol.* 2020;114:104670.
105. Tahsin T, Wansi JD, Al-Groshi A, et al. Cytotoxic properties of the stem bark of *Citrus reticulata* Blanco (Rutaceae): cytotoxic property of stem bark of citrus *reticulata* Blanco. *Phytother Res.* 2017;31:1215-1219.
106. Kaushal S, Kalia A, Kaur V. Proximate, mineral, chemical composition, antioxidant and antimicrobial potential of dropped fruits of citrus *reticulata* Blanco. *J Food Meas Charact.* 2022;16:4303-4317.
107. Mizuno H, Yoshikawa H, Usuki T. Extraction of nobiletin and tangeretin from peels of Shekwasha and Ponkan using [C₂ mim][(MeO)(H)PO₂] and centrifugation. *Nat Prod Commun.* 2019;14:1934578X1984581.
108. Yaqoob M, Aggarwal P, Babbar N. Extraction and screening of kinnow (*Citrus reticulata* L.) peel phytochemicals, grown in Punjab, India. *Biomass Convers Bio-refinery.* 2023;13:11631-11643.
109. Uddin TM, Chakraborty AJ, Khusro A, et al. Antibiotic resistance in microbes: history, mechanisms, therapeutic strategies and future prospects. *J Infect Public Health.* 2021;14:1750-1766.
110. Das R, Rauf A, Mitra S, et al. Therapeutic potential of marine macrolides: an overview from 1990 to 2022. *Chem Biol Interact.* 2022;365:110072.
111. Kapoor G, Saigal S, Elongavan A. Action and resistance mechanisms of antibiotics: a guide for clinicians. *J Anaesthesiol Clin Pharmacol.* 2017;33:300-305.
112. Yao X, Zhu X, Pan S, et al. Antimicrobial activity of nobiletin and tangeretin against *Pseudomonas*. *Food Chem.* 2012;132:1883-1890.
113. Jayaprakasha GK, Negi PS, Sikder S, Mohanrao LJ, Sakariah KK. Antibacterial activity of citrus *reticulata* peel extracts. *Z Für Naturforschung C.* 2000;55:1030-1034.
114. Memariani Z, Moeini R, Hamed SS, Gorji N, Mozaffarpur SA. Medicinal plants with antithrombotic property in Persian medicine: a mechanistic review. *J Thromb Thrombolysis.* 2018;45:158-179.
115. Gupta N, Zhao Y-Y, Evans CE. The stimulation of thrombosis by hypoxia. *Thromb Res.* 2019;181:77-83.
116. Chakraborty AJ, Uddin TM, Matin Zidan BMR, et al. Allium cepa: a treasure of bioactive phytochemicals with prospective health benefits. *Evid Based Complement Alternat Med.* 2022;2022:4586318.
117. Lu WJ, Lin KC, Liu CP, et al. Prevention of arterial thrombosis by nobiletin: in vitro and in vivo studies. *J Nutr Biochem.* 2016;28:1-8.
118. Vaiyapuri S, Ali MS, Moraes LA, et al. Tangeretin regulates platelet function through inhibition of phosphoinositide 3-kinase and cyclic nucleotide signaling. *Arterioscler Thromb Vasc Biol.* 2013;33:2740-2749.
119. Marder VJ. Recombinant streptokinase: opportunity for an improved agent. *Blood Coagul Fibrinolysis.* 1993;4:1039-1040.
120. Wu D-H, Shi G-Y, Chuang W-J, et al. Coiled coil region of streptokinase γ -domain is essential for plasminogen activation. *J Biol Chem.* 2001;276:15025-15033.
121. Shinde UA, Phadke AS, Nair AM, Mungantiwar AA, Dikshit VJ, Saraf MN. Membrane stabilizing activity—a possible mechanism of action for the anti-inflammatory activity of *Cedrus deodara* wood oil. *Fitoterapia.* 1999;70:251-257.
122. Jin J, Lv X, Wang B, et al. Limonin inhibits IL-1 β -Induced inflammation and catabolism in chondrocytes and ameliorates osteoarthritis by activating Nrf2. *Oxid Med Cell Longev.* 2021;2021:e7292512.

123. Witschi HP. Enhanced tumour development by butylated hydroxytoluene (BHT) in the liver, lung and gastro-intestinal tract. *Food Chem Toxicol.* 1986;24: 1127-1130.
124. Oguntibeju OO. Medicinal plants with anti-inflammatory activities from selected countries and regions of Africa. *J Inflamm Res.* 2018;11:307-317.
125. Sarmiento-Neto J, Do Nascimento L, Felipe C, De Sousa D. Analgesic potential of essential oils. *Molecules.* 2015;21:E20.
126. Nirmal SA, Pal SC, Mandal SC, Patil AN. Analgesic and anti-inflammatory activity of β -sitosterol isolated from *Nyctanthes arbortristis* leaves. *Inflammo-pharmacology.* 2012;20:219-224.
127. Zewdie KA, Bhounik D, Wondafrash DZ, Tuem KB, Tuem KB. Evaluation of in-vivo antidiarrhoeal and in-vitro antibacterial activities of the root extract of *Brucea antidysenterica* JF mill (Simaroubaceae). *BMC Complement Med Ther.* 2020;20:11.
128. Naher S, Aziz MA, Akter MI, Rahman SMM, Sajon SR, Mazumder K. Anti-diarrheal activity and brine shrimp lethality bioassay of methanolic extract of *Cordyline fruticosa* (L.) A. Chev. leaves. *Clin Phytoscience.* 2019;5:15.
129. Panganamala RV, Miller JS, Gwebu ET, Sharma HM, Cornwell DG. Differential inhibitory effects of vitamin E and other antioxidants on prostaglandin synthetase, platelet aggregation and lipoxidase. *Prostaglandins.* 1977;14: 261-271.
130. Cajas YN, Cañón-Beltrán K, Ladrón de Guevara M, et al. Antioxidant nobiletin enhances oocyte maturation and subsequent embryo development and quality. *Int J Mol Sci.* 2020;21:5340.
131. Wang M, Meng D, Zhang P, et al. Antioxidant protection of nobiletin, 5-demethylnobiletin, tangeretin, and 5-demethyltangeretin from citrus peel in *Saccharomyces cerevisiae*. *J Agric Food Chem.* 2018;66:3155-3160.